Essentials of CT Image Interpretation

14

Davide Caramella, Matteo Revelli, and Alessandro Villa

Contents

D. Caramella (✉)
Diagnostic and Interventional Radiology,
Department of Translational Research and Advanced Technologies in Medicine and Surgery, University of Pisa, Pisa, Italy
e-mail: davide.caramella@unipi.it

M. Revelli
Department of Diagnostic Imaging and Laboratory Medicine,
AUSL di Reggio Emilia – IRCCS, Reggio Emilia, Italy

A. Villa
Unit of Radiology 2, ASL 5 "Spezzino", Sarzana, La Spezia, Italy

D. Volterrani et al. (eds.), *Nuclear Medicine Textbook*, https://doi.org/10.1007/978-3-319-95564-3_14

Learning Objectives

- Discuss the non-enhanced and contrast-enhanced acquisition techniques required to correctly interpret a CT exam.
- Describe the principal thoracoabdominal lesions with an organ-oriented approach.
- Formulate a differential diagnosis on the basis of the attenuation and contrast enhancement features of thoracoabdominal lesions.

14.1 Introduction

The combination of information derived from positron-emission tomography (PET) and anatomic information from computed tomography (CT) provides an important tool in the management of patients with cancer and cardiovascular disease. To effectively utilize CT images, knowledge of normal anatomic features and common pathological alterations that can be assessed with CT is required. This chapter will focus on the principles of performing and interpreting CT images.

14.2 Visualization and Elaboration of CT Images

Multidetector helical CT scanners recording ≥64 slices are the standard for image acquisition. In common clinical practice, a reconstructed slice thickness of 5 mm is employed for image visualization on the axial plane. Thinner slices of 0.625 mm can be acquired to improve image quality and allow better assessment of anatomic details. The most frequently used reconstructions are multiplanar reconstruction (MPR), volume rendering (3D) reconstruction, and also maximum intensity projection (MIP) or minimum intensity projection (MinIP) reconstructions.

14.2.1 Multiplanar Reconstruction (MPR)

Multiplanar reconstructions are bidimensional images generated using data from acquired in the helical dataset. Coronal, sagittal, oblique, and curved reconstructions are obtained interpolating data derived from adjacent voxels (Fig. 14.1a). They can be useful to evaluate the relationships between a neoplastic mass and the surrounding structures, and they have a role in advanced CT applications, such as vessel evaluation in CT angiography.

14.2.2 Maximum Intensity Projection (MIP) and Minimum Intensity Projection (MinIP)

These are volume rendering techniques that allow definitions of volumes of interest (VOI): images are obtained by projecting the VOI on a visualization plane selecting high Hounsfield numbers for MIPs and low Hounsfield numbers for MinIPs, providing an optimal contrast. MIPs are mainly used for CT angiography applications and for the evaluation of pulmonary parenchyma (Fig. 14.1b), while MinIPs play a role in the study of air-filled structures such as the tracheobronchial tree.

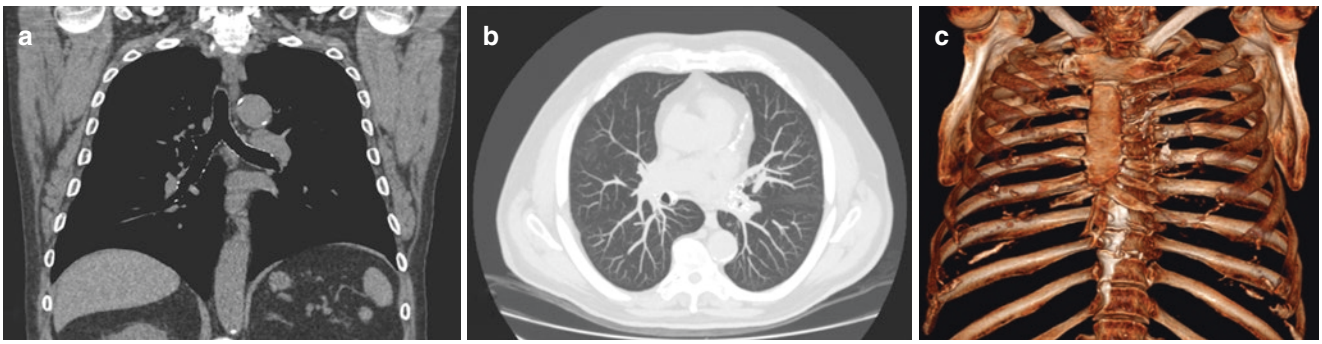

Fig. 14.1 Multiplanar reconstruction on the coronal plane of the chest (**a**); maximum intensity projection reconstruction on the axial plane for the evaluation of pulmonary parenchyma and vessels (**b**); 3D volume rendering of the chest for the evaluation of the bony structures of the chest (**c**)

14.2.3 3D Surface Rendering

It is represented by a surface image providing a realistic three-dimensional depiction of a structure of interest inside the acquired volume (Fig. 14.1c). 3D surface rendering has the advantage of immediate and easy interpretation for surgeons during surgical planning and plays a role in virtual endoscopy, providing reconstructions that allow interactive navigation.

Key Learning Points

- Helical CT represents the standard for image acquisition, and modern multidetector scanners can improve image quality by using various image algorithms.
- Multiplanar reconstruction (MPR), volume rendering (3D) reconstruction, and maximum intensity projection (MIP) or minimum intensity projection (MinIP) reconstructions are widely used in diagnostic imaging to obtain additional information and for advanced applications, such as CT angiography and virtual endoscopy.

14.3 Image Analysis and Interpretation

14.3.1 Density Values and Hounsfield Units (HU)

CT numbers are normalized values of the calculated X-ray absorption coefficient of a voxel in a CT image, expressed in Hounsfield units (HU); they play a central role in the characterization of different tissues, since air, fat, fluids, and blood have different attenuation values. Depending on the CT number of voxels, their corresponding pixels are defined as hyperdense, isodense, or hypodense with regard to surrounding tissues. CT images can be displayed using different gray level settings, the so-called windows, in order to improve contrast between structures.

On non-enhanced CT (NECT, CT images acquired without the use of iodinated contrast material), specific tissue components can be characterized based on native attenuation values.

Air collections can be easily identified using a pulmonary window that is routinely used for the assessment of lung parenchyma. This can prove useful also in the evaluation of extrathoracic areas, for example, to detect the presence of free air in the peritoneal cavity. Windows settings commonly used for the evaluation of parenchymas and soft tissues may fail to identify gaseous areas, or low attenuation fat areas may be mistakenly interpreted as air (Fig. 14.2): a CT number < -150 HU in soft tissues is pathognomonic for the presence of gas. The search for air must always be carried out in the study of trauma patients or in cases of suspected perforation, and it should be remembered that the air tends to settle in the upper parts of the body. The presence of air inside a fluid mass should raise the suspicion of an abscess.

Fat presents a density value of about -100 HU, and adipose infiltration of various tissues (liver, pancreas, muscles) has to be suspected when a reduction of expected density values is noticed. The presence of fat in a lesion is important to establish the diagnosis in many diseases, and its percentage may vary according to the type of lesion: a mass entirely composed of adipose tissue is typically a lipoma, while the presence of other solid components may suggest the diagnosis of a more aggressive lesion.

Regarding fluid, pure *water* has a density of 0 HU, although – due to technical factors and variable composition of bodily fluids – values ranging from -10 to 10 HU are consistent with watery fluid. Denser fluids can demonstrate higher attenuation values possibly overlapping with those of soft tissues; for these reasons, often a cystic lesion can be safely distinguished from a solid lesion only after the administration of contrast material.

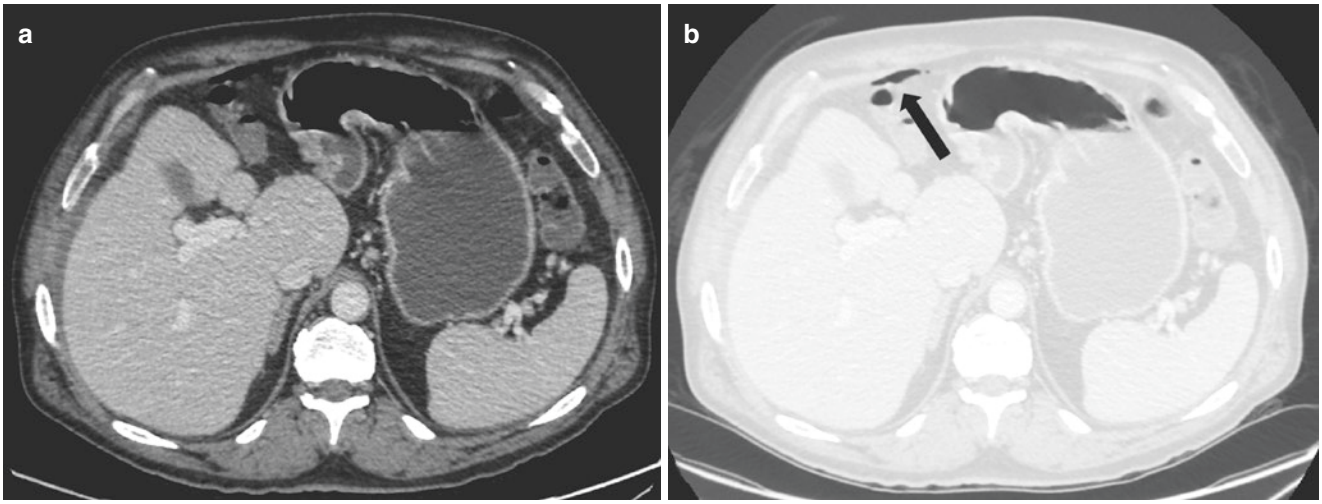

Fig. 14.2 CT of a 55-year-old man with abdominal pain. On the soft tissue window (**a**), the free air collection may be difficult to depict, but the use of the pulmonary window (**b**) makes it easy to identify the air collection adjacent to the stomach (arrow)

Blood attenuation is higher than water and depends on the concentration of hemoglobin; in case of anemia, the blood may appear less hyperdense. Hemorrhage density is influenced by the time passed since the onset, the presence of clots, and the site of bleeding: a recent hemorrhage is typically seen as a hyperdense collection (>80 HU). Subacute hemorrhage tends to show a reduction of blood attenuation due to lysis of red cells and to hemoglobin reabsorption. MRI is more sensitive in estimating the age of a hemorrhage, since blood has specific T1 and T2 signal characteristics correlating with the stage of evolution.

A density higher than 100 HU suggests the presence of calcific deposits. *Calcifications* may be the consequence of many pathological processes, and their presence may be indicative of the benign or malignant nature of various lesions, with specific features in the various body districts. *Metallic* foreign materials show the highest attenuation values, and they are often associated with peculiar imaging artifacts.

14.3.2 Morphological Evaluation of CT Images

The accuracy of image evaluation is related to technical aspects (i.e. pixel size, reconstruction algorithm), and is influenced by acquisition parameters: as a consequence of incorrect acquisition protocols, some lesions can be difficult to measure, and a comprehensive morphological evaluation cannot always be achieved.

Size evaluation is one of the most reproducible measurements in CT images: focal lesions are usually measured by tracing two perpendicular lines along the two largest diameters of the lesion, possibly using MPR to obtain the most suitable planes for the measurements (Fig. 14.3); furthermore, a volumetric assessment can be made, by using multiplane measurements and automated software.

When considering the margins of a focal lesion, the difference in tissue attenuation can help identify tissue borders; well defined margins are often associated with benign lesions, whereas ill-defined margins may be a sign of infiltration.

Sometimes it is difficult to attribute a lesion uniquely to a specific organ, especially in the absence of adipose cleavage plans that allow a clear separation from the adjacent organs: in such cases, the angle between the lesion and the organ can point to the diagnosis, since an obtuse angle indicates the origin of the lesion from the organ in question, while an acute angle suggests an extrinsic lesion.

A key feature to be evaluated is the differentiation between expansive lesions that tend to displace and compress the adjacent organs and infiltrative lesions that have ill-defined contours and extend to adjacent structures: in particular, vascular infiltration represents a key element in the staging of many cancers, often affecting surgical management, since a tumor that surrounds a vessel for more than 50% of its circumference is usually consistent with vascular infiltration.

In some cases it may not be easy to distinguish between a tumor and an inflammatory process, and the evaluation of clinical parameters and laboratory tests should be the basis for the differential diagnosis. In particular, the most challenging situations occur in the lungs (differential diagnosis of pneumonia and bronchial-alveolar carcinoma), in the pancreas (chronic pancreatitis vs adenocarcinoma), and in general in the follow-up of oncologic patients when it is indispensable to distinguish between recurrence and surgery-related fibrosis.

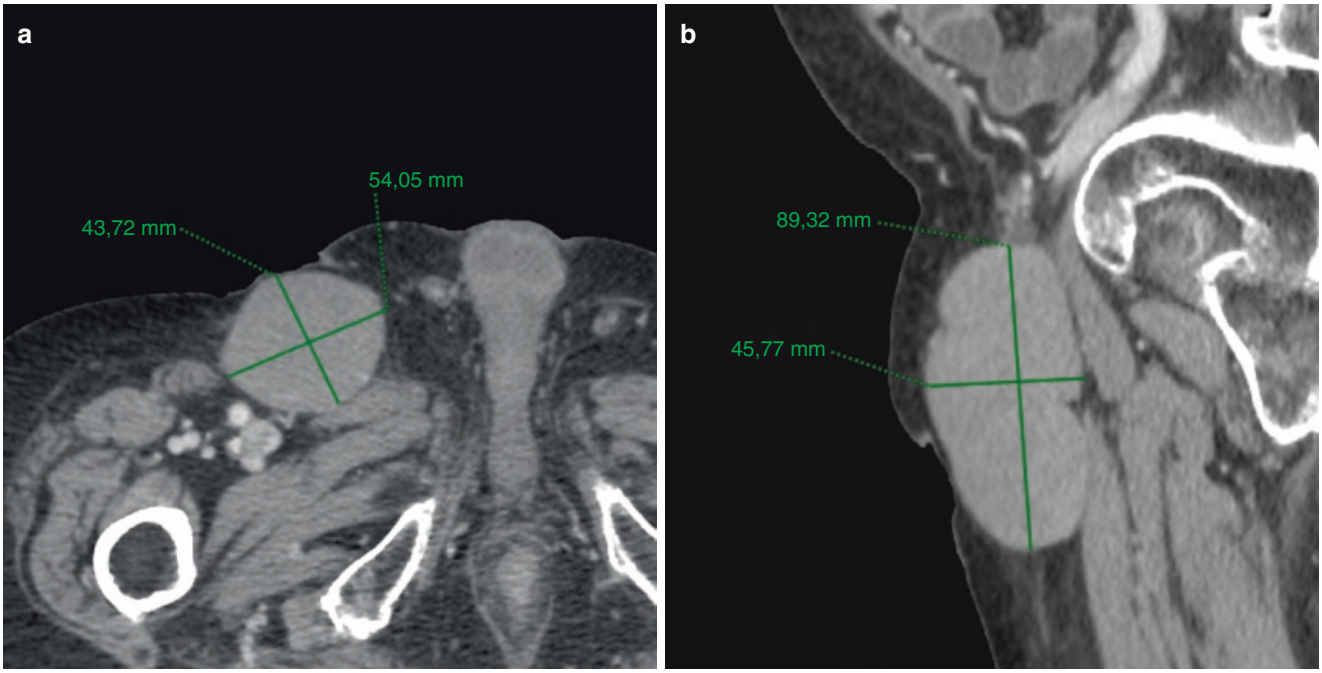

Fig. 14.3 Use of MPR reconstructions to obtain the largest diameters of an inguinal enlarged lymph node. On the axial plane (**a**), we can measure the largest latero-lateral diameter, while on the sagittal plane (**b**), we have a better and more reliable depiction of anteroposterior and craniocaudal diameters

14.3.3 Patterns of Contrast Enhancement

Contrast enhanced CT (CECT) is useful to detect and characterize lesions in different anatomic sites. Multiphase CT protocols are routinely used and tailored on the clinical indication; they may include a non-enhanced CT scan followed by contrast-enhanced CT acquisitions at various intervals after contrast administration.

NECT is useful to detect stones in the urinary tract and to differentiate cystic lesions from solid lesions (i.e., renal cyst from solid neoplasm), hematomas and hemorrhagic cysts from clear fluid collections and simple cysts (between 0 and 15 HU is fluid collection; more than 60 HU can be considered as hemorrhagic), and fat-containing lesions (density is <0 UH) such as lipomas, renal angiomyolipoma, and lipid-rich adrenal adenoma (density <10 HU is sufficient for diagnosis) from other solid lesions. NECT is also important to evaluate the amount of contrast enhancement when compared with CECT acquisitions.

CECT scans are usually acquired at standardized times after contrast administration to evaluate dynamic patterns of enhancement that may help in establishing a definite diagnosis. Since contrast enhancement kinetics may differ among different patients, owing to both physiological and disease-related factors, a bolus-tracking technique is often used to ensure optimal enhancement.

Bolus tracking is performed with the application of dedicated software that allows a measurement at short time intervals of attenuation values in a region of interest (ROI) usually placed at different level of the aorta depending on clinical indications. Image acquisition automatically starts when a predefined HU value is reached in the ROI.

A multiphase contrast enhancement CT protocol consists of various acquisitions that may include NECT (if needed), early and late arterial phase, portal phase, equilibrium phase, and delayed phases.

The early arterial phase is obtained at the time of maximum vessel enhancement (usually between 25 and 30 s after injection of contrast), and it is used to evaluate the arterial vessels in CT angiography. Late arterial phase is acquired about 10–15 s later and is commonly used for the detection of hypervascular tumors and for the assessment of organs such as the pancreas. Venous portal phase starts about 30–35 s after the end of the late arterial phase and is very useful in the evaluation of parenchymal organs. The assessment of contrast enhancement in late arterial and venous portal phase is the mainstay to characterize solid lesions based on the recognition of specific enhancing patterns. Equilibrium phase is obtained at 3–5 min after administration of contrast, and it is commonly acquired in liver evaluation protocols to aid in lesion characterization.

The iodinated contrast material is normally eliminated by the kidneys, and it progressively opacifies the urinary collecting system. Post-contrast acquisition in the delayed phases, between 7 and 10 min after contrast administration, allows the evaluation of the urinary system filled by

highly concentrated contrast material, which can be useful to depict anatomic details, demonstrate intraluminal pathologies, or other abnormalities of the urinary tract.

Parenchymal focal lesions may have a basal density at NECT that makes them difficult to distinguish from the adjacent parenchyma; therefore, their vascular kinetics on CECT is often a key element for guiding differential diagnosis.

Based on contrast enhancement, focal lesion can be divided as follows:

- *Cystic lesions* have variable attenuation values on NECT based on their fluid composition, and do not exhibit significant contrast enhancement on CECT. Small round cystic lesions can present an apparent increase in attenuation values in the central portion after contrast administration called *pseudoenhancement*, an artifactual phenomenon due to the particular pattern of X-ray attenuation by surrounding enhancing parenchyma. For this reason, a limited increase in attenuation after contrast (up to 15 HU) can still be consistent with a cystic lesion. The presence of enhancing solid parts within a cyst should raise the suspicion of a complex cystic lesion that could be neoplastic in nature.
- *Hypervascular lesions* exhibit a stronger enhancement compared to the surrounding parenchyma during the late arterial phase: typical examples of hypervascular tumors are hepatocellular carcinoma, renal carcinoma, and hypervascular metastases. Lesions with a hypervascular behavior may show various patterns of contrast enhancement that can range from homogeneously enhancing lesion to marked heterogeneous masses. A particular pattern of contrast enhancement is represented by "rim enhancement" which consists of a continuous peripheral vascularization with a relative hypovascular central portion. Rim enhancement is a typical finding in liver metastases. In portal venous and equilibrium phases, hypervascular lesions can demonstrate variable enhancement compared to late arterial phase; the washout phenomenon is a frequent occurrence in malignant hypervascular lesions, and it is seen as a reduced attenuation relative to surrounding parenchyma following the maximum enhancement.
- *Hypovascular lesions* exhibit less vascularity than the adjacent parenchyma resulting in hypo-attenuation areas typically seen in portal venous and equilibrium phases.

14.3.4 Artifacts and Pitfalls in CT Imaging

CT images may suffer from several kinds of artifacts. The best known is the metal artifact, due to the fact that metal causes high Xray scatter that limits the evaluation of surrounding tissues (Fig. 14.4). In addition, beam-hardening artifacts can cause dark streaks between dense objects (bones); motion or respiratory artifacts determine image blurring, and detector size may cause linear and nonlinear partial volume artifacts. Contrast media can also be a source of pitfalls; as an example, an incomplete opacification of venous vessels that can be observed in the arterial phase may occasionally mimic thrombosis.

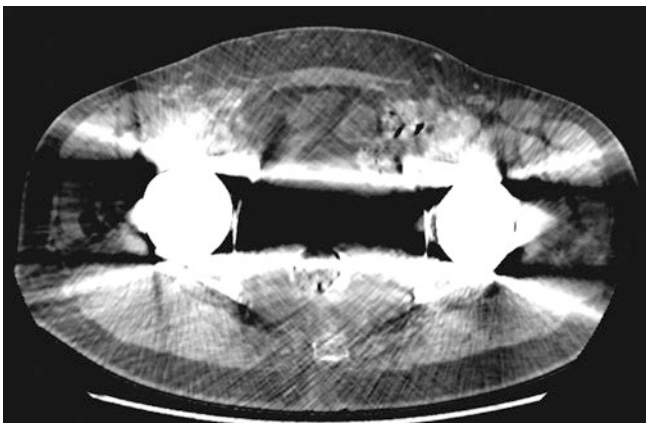

Fig. 14.4 Metal artifact, due to the presence of bilateral hip prostheses

Key Learning Points

- Density characteristics, expressed in Hounsfield units (HU), play a central role in the identification of different tissues, since air, fat, watery fluids, and fresh blood have specific attenuation values.
- Several morphological criteria, such as size and margins, can be used in the assessment of CT images.
- Different image windowing (lung, abdomen, mediastinum) can lead to a better evaluation of different lesions in various organs.
- Tumors may have specific patterns of contrast enhancement, and the knowledge of such characteristics during the different phases (arterial, portal, venous) is essential to reach the correct diagnosis.
- Based on contrast enhancement, focal lesions can be divided into cystic, hypovascular, and hypervascular.
- Recognition of CT artifacts is fundamental to distinguish them from pathological entities.

14.4 Neck

CT is a widely used imaging technique for the evaluation of the neck; however, in some cases, the better contrast resolution between soft tissues provided by MRI can help delineate

anatomical structures and characterize pathological conditions. CT is the modality of choice for the study of the lower part of the neck, especially in debilitated and fragile patients, such as those in intensive care units. Furthermore, CT may be preferable in patients with suspicion of osseous involvement, due to its ability to evaluate the cortical bone. A short overview of principal cystic and solid lesion of the neck will be provided in this paragraph.

14.4.1 Cystic Lesions

A wide variety of cystic lesions may be found in the neck, and the knowledge of spatial and fascial neck anatomy is essential in order to formulate a correct differential diagnosis. *Thyroglossal duct cysts* appear as uniloculated fluid masses in the anterior neck, with thin walls and slight peripheral enhancement. Wall focal thickenings or protruding nodules may indicate malignant evolution. *Branchial cleft cysts* are displayed as unilateral well-defined hypodense masses; walls may thicken in case of infection, and their enlargement may lead to a compression of surrounding structures. *Thymic cysts* are rare and may be seen anywhere between the mandibular angle and the mediastinum: CT shows a fluid uni- or multiloculated mass with elongated shape next to the carotid space; their size may reach 20 cm. *Cystic lymphangioma* presents as a mass characterized by multiple ill-defined cystic spaces, usually located in the posterior cervical space; it may show increased density when infected. Other rare cystic lesions of the neck include dermoid and epidermoid cysts, laryngocele, and Tornwaldt cysts.

14.4.2 Neoplastic Lesions

A wide variety of benign tumors may affect the neck, including neurogenic tumors, such as schwannomas and neurofibromas, and mesenchymal tissue tumors, such as lipomas, hemangiomas, and desmoid or fibrous tumors.

Regarding malignant lesions, the presence of lymph node metastasis is very important for prognostic stratification. CT can evaluate nodal involvement in staging head and neck tumors, but more accurate techniques are currently being developed for a more precise presurgical evaluation.

Malignant tumors of the neck are:

- *Nasopharyngeal carcinoma*
  Mainly represented by squamocellular carcinomas with preferential involvement of the lateral walls (fossa of Rosenmuller). CT plays an important role in the evaluation of deep-layer invasion, skull base erosions with intracranial extension, and perineural spread (along the mandibular nerve).
- *Oropharyngeal carcinoma*
  They are usually more aggressive and less differentiated than nasopharyngeal carcinomas, with an insidious onset, often presenting with symptoms only in advanced and metastatic stage. They can originate from the basis of the tongue, from the tonsillar region (Fig. 14.5) or from the posterior wall. CT can delineate the relationship with the surrounding structures as well as the invasion of neurovascular bundle and soft tissue layers.
- *Oral cavity carcinoma*
  They are often asymptomatic and may involve the lips, the floor of the mouth, the oral segment of the tongue, the oral mucosa or gums, and the palate. CT plays a role in the staging of these tumors, depicting mucosal, bone, perineural, and deep invasion.
- *Hypopharyngeal carcinoma*
  They usually develop in the submucosal layer, and CT may identify tumors that are not visible at endoscopy, providing information such as tumor volume (important for treatment planning), contralateral extension, cartilaginous and neurovascular invasion, and extralaryngeal spread.
- *Laryngeal carcinoma*
  They are usually squamocellular tumors related to alcohol and tobacco abuse; they often develop in the submucosa, so endoscopy has a limited role. They can be surrounded by a perilesional inflammation, so CT may overestimate their size. They can be classified as supraglottic, glottic,

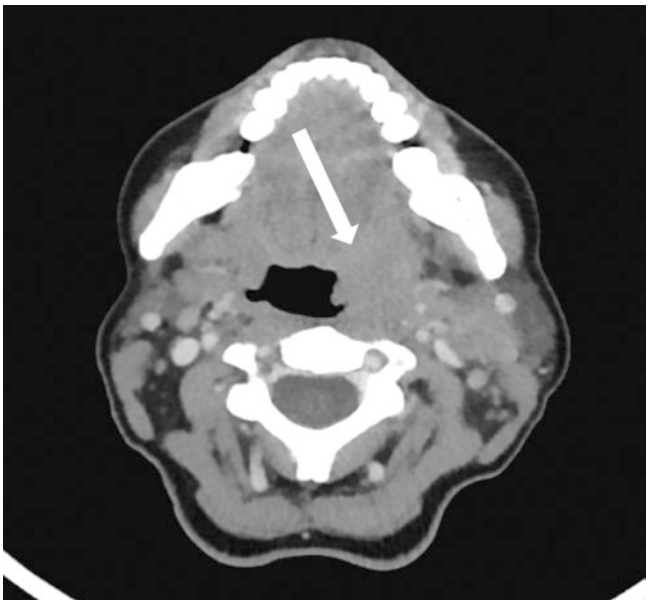

Fig. 14.5 Oropharyngeal carcinoma originating from the left tonsillar region (arrow)

and subglottic tumors, each one with specific TNM staging, spread pattern, and lymphatic drainage. CT may indicate their volume, the invasion of different planes and the extralaryngeal spread.
- *Lymphomas*
- *Mesenchymal tissue and neurogenic malignant tumors*

14.4.3 Infectious Diseases

CT plays a role in the evaluation of cases in which there is no response to antibiotic therapy and it can help in differentiation of complicated forms. *Cellulitis* may present as a soft tissue mass showing marked enhancement after the administration of contrast material, with edematous thickening of the skin and obliteration of fascial and fat layers. Air collection indicates the presence of gas-producing bacteria. *Suppurative lymphadenitis* is characterized by node enlargement showing signs of colliquative necrosis and surrounding edema. *Abscesses* are hypodense masses with capsular enhancement. Complications may include septic thrombosis of the jugular veins and mediastinitis. Other granulomatous diseases, such as tuberculosis, sarcoidosis, and cat scratch disease, or conditions like infectious mononucleosis or Castleman disease may all cause nodal involvement.

14.4.4 Thyroid and Parathyroid Gland Pathologies

CT is not the modality of choice for the study of the thyroid; however, during a CT examination for other indications, important information about the thyroid gland can be collected. Furthermore, an accurate evaluation of the thyroid function should be performed before the administration of iodinated contrast media.

A *goiter* is a benign enlargement of the thyroid gland, often asymmetric, characterized by mixed solid and cystic nodules; calcifications and hemorrhage may be present, and contrast enhancement is usually patchy.

Benign thyroid nodules are frequent, mainly represented by colloid cysts. *Follicular adenomas* appear as hyperdense well-defined masses, and they are virtually indistinguishable from a nodular goiter. *Papillary carcinoma* is the most common thyroid tumor, and it can be multifocal or bilateral, with cystic, hemorrhagic, or calcific components. *Follicular carcinomas* can be both capsulated and diffusely infiltrating, with frequent invasion of vascular structures. *Anaplastic carcinoma* is more common in the elderly, and it can show calcification and necrotic areas, with invasion of surrounding structures (Fig. 14.6). *Medullary carcinoma* is rare and may be part of a MEN syndrome. CT findings of thyroid carcinomas are unspecific, and overlapping features between benign and malignant tumors are frequent and other investigations are often necessary to achieve a correct diagnosis.

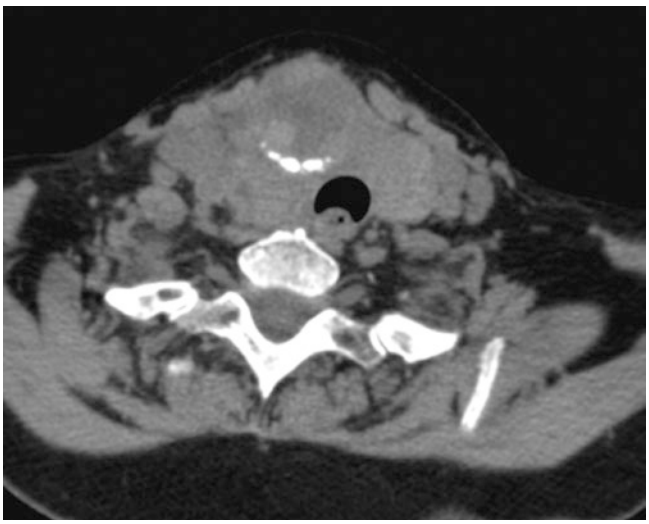

Fig. 14.6 Anaplastic thyroid carcinoma appearing as an ill-defined mass showing calcification and necrotic areas, with invasion of the surrounding structures and dislocation of the trachea and of the other upper mediastinal structures

Key Learning Points
- CT is a widely used imaging technique for the evaluation of the lower part of the neck, especially in fragile patients and for the evaluation of osseous involvement.
- A wide variety of cystic lesions may be found in the neck, and the knowledge of neck anatomy is essential to reach a correct diagnosis.
- CT can evaluate nodal involvement in staging head and neck tumors.
- CT plays a role in the evaluation of infectious neck disease and can help in diagnosing complicated forms.

14.5 Lungs and Airways

If plain radiographs still represent the first diagnostic modality for the evaluation of the chest, CT is the most sensitive technique for the assessment of pulmonary parenchyma, playing a central role in diagnosis, staging, and follow-up of pulmonary and mediastinal cancers. High-resolution CT can be useful to evaluate the presence of diffuse lung disease, allowing an accurate analysis of pulmonary interstitium. Furthermore, CT can play a role in the evaluation of airways,

and it can be used to guide interventional procedures, such as biopsies or drainages. In this paragraph, we will provide an easy and immediate guide to the interpretation of frequent entities such as the solitary pulmonary nodule, infections and interstitial diseases.

14.5.1 Solitary Pulmonary Nodule: CT Image Interpretation

A solitary pulmonary nodule is defined as a rounded, well-defined opacity with a diameter less or equal to 3 cm, without hilar or mediastinal interface and presenting without concomitant lymphadenopathies, atelectasis, or pleural effusion (Fig. 14.7). Differential diagnosis and management of this entity is a matter of debate and depends on whether the lesion is malignant, so it is crucial to establish imaging features to distinguish between benign and malignant nodules. We will review the main features that need to be considered in the diagnostic approach to the solitary pulmonary nodule.

- *Size, location, and volume*
  Lesions with a diameter larger than 3 cm are defined as masses and must be considered as malignant until proven otherwise. Comparison with previous imaging studies is mandatory to establish the size evolution of the lesion: dimensional stability over a 2-year period is considered a benignity criterion. Peripheral subpleural location is also considered indicative of benignity.
- *Shape and margins*
  Polygonal shape and high three-dimensional ratio (indicating that the lesion is relatively flat) are considered benign features. Smooth margins are usually associated with benign nodules, while scalloped or lobulated margins may indicate a suspicious lesion; the *corona radiata sign*, a thin, irregular, and spiculated edge extending to the periphery of the nodule, is frequently associated with malignant lesions.
- *Calcifications*
  There are several patterns of benign calcifications, including diffuse, central, laminated, and popcorn calcifications, often seen in granulomatous diseases; calcifications patterns not belonging to these groups should not be considered as a sign of benignity.
- *Nodule composition*
  Nodules containing a ground-glass component are more likely to be malignant, and the odds rise with mixed solid and ground-glass components, while pure solid or pure ground-glass nodules have lower rates of malignancy. The *air bronchogram sign* can also be associated with malignant pulmonary nodules (most commonly bronchoalveolar cell carcinoma and adenocarcinoma).
- *Contrast enhancement*
  Increase of density equal or less than 15 HU is considered index of benignity. Higher enhancement, along with other

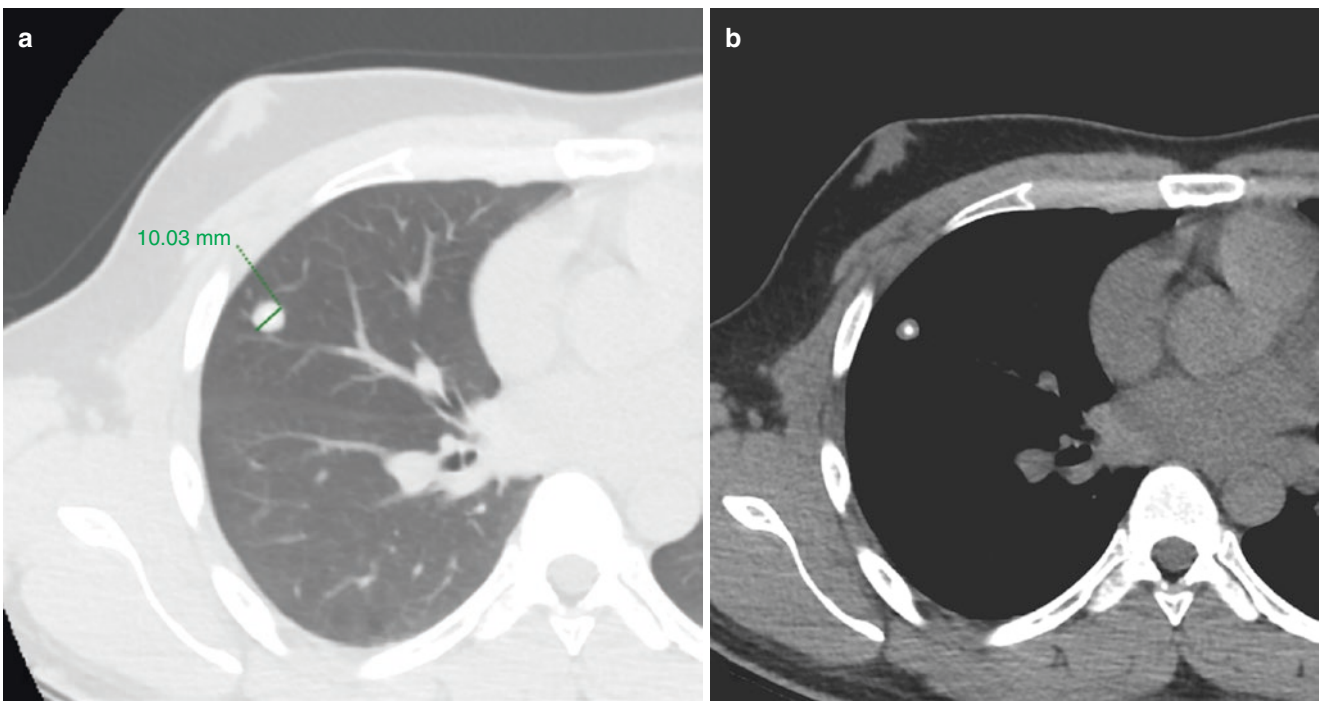

Fig. 14.7 Solitary pulmonary nodule (10 mm) in the middle lobe (pulmonary window in **a**). This nodule was an incidental finding. Soft tissue window shows a central calcification (**b**). According to guidelines, a 12-month follow-up was performed

Table 14.1 Differential diagnosis of pulmonary nodules

Granulomatous diseases	Tuberculosis
	Histoplasmosis
	Sarcoidosis
Benign tumors	Hamartomas
	Pulmonary pseudotumors
Malignant tumors	Peripheral bronchial carcinoma
	Bronchoalveolar carcinoma
	Metastases (usually multiples)
	Carcinoids
	Kaposi sarcoma
	Lymphoma
Other conditions	Septic embolism
	Intrapulmonary lymph nodes
	Arteriovenous malformations
	Round atelectasis

suspicious findings, requires further diagnostic work-up and histological assessment.

The Fleischner Society periodically updates guidelines for the management of pulmonary nodules, considering characteristics such as size, density, and location, stratified for high- and low-risk patients. The 2017 updated guidelines can be consulted online at https://fleischnersociety.org. About 50% of pulmonary nodules that undergo surgery are benign. A schematic differential diagnosis of pulmonary nodules is reported in Table 14.1.

14.5.2 Infectious Diseases

Pulmonary infectious diseases usually do not require CT evaluation. However, CT can help identify complications or exclude predisposing conditions and monitor the progression of disease and the therapeutic response. Clinical features can point to an etiologic diagnosis, for example in debilitated or immunocompromised patients.

Typical CT appearance of *bacterial pneumonia* includes areas of parenchymal consolidation with air bronchogram (Fig. 14.8): these opacities can be focal or multiple, merging to segmentary or lobar involvement of air spaces. Central excavations and abscesses may develop. *Atypical nonviral pneumonias* (i.e., caused by *M. pneumoniae*) are characterized by centrilobular nodules ("tree in bud," see the chapter Diffuse Lung Disease: Patterns of Interstitial Involvement), air trapping phenomena, and mosaic attenuation, in association with ground-glass opacities and lobular parenchymal consolidations. *Viral infections* show areas of patchy parenchymal attenuation and diffuse "tree in bud" aspects. CT features of *tuberculosis* may include acinar opacities with peribronchial distribution; nodular involvement of all pulmonary parenchyma due to miliary spread; excavations with thin or thick walls, and enlarged mediastinal lymph nodes with central necrosis and intense peripheral rim enhancement.

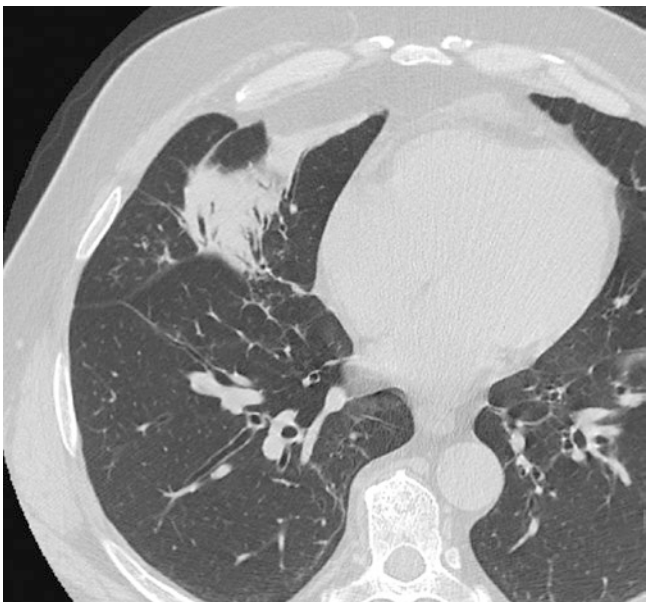

Fig. 14.8 Focal area of parenchymal consolidation with "air bronchogram" sign in the middle lobe, due to bacterial pneumonia

14.5.3 Diffuse Lung Diseases: Patterns of Interstitial Involvement

To understand the pathological alterations of interstitial lung diseases, it is important to know the anatomic organization of the broncho-vascular structures (large bronchi, pulmonary vessels, and central interstitium) and of the secondary lobule, the most peripheral parenchymal unit in which peripheral interstitium supports the fusion between airways and vascular structures. Interpretation of interstitial diseases is mainly based on the type and degree of involvement of the secondary lobule. Vessels appear on CT images as linear opacities (or circular one when viewed in section), that branch dichotomously from the center to the periphery, side by side with the bronchial structures; on the other side, pulmonary veins have a distinct course and show monopodic confluence of the minor branches into the major ones. The *secondary lobule* measures about 1–2 cm and contains 5–15 pulmonary acini; it is supplied by a terminal bronchiole paired with a centrilobular artery (centrilobular area), while pulmonary veins and lymphatics are located in the peripheral interlobular septa (perilymphatic area).

CT interpretation of interstitial involvement requires a structured approach considering the dominant pattern

Table 14.2 Differential diagnosis of diffuse lung disease according to distribution within the lung

Upper distribution	Sarcoidosis, silicosis, pneumoconiosis, centrilobular emphysema, chronic hypersensitivity pneumonia, Langerhans cell histiocytosis
Lower distribution	Pulmonary edema, panlobular emphysema, aspiration-related conditions, usual interstitial pneumonia
Central distribution	Sarcoidosis, bronchitis, cardiogenic pulmonary edema
Peripheral distribution	Chronic eosinophilic pneumonia, hematogenous metastasis, usual interstitial pneumonia, organizing pneumonia

(reticular, nodular, high attenuation, low attenuation), its location within the secondary lobule (i.e., centrilobular or perilymphatic), its distribution in the lung (upper vs lower lobe, central vs peripheral location, Table 14.2), and the presence of additional findings such as pleural effusion or enlarged lymph nodes.

The *reticular pattern* is characterized by septal thickening or can be related to advanced fibrosis:

- *Thickening of the interlobular septa*
  Fluid, fibrous tissue or cell infiltration can lead to septal thickening and subsequent reticular opacity, which can be smooth (i.e., in interstitial pulmonary edema) or nodular (i.e., in sarcoidosis).
- *Honeycombing*
  It is represented by microcystic spaces surrounded by thickened bronchiolar structures due to fibrous evolution, and it is the typical pattern of usual interstitial pneumonia (UIP).

The *nodular pattern* can be divided into three main classes on the basis of the distribution of the nodules (Table 14.2), which includes:

- *Centrilobular distribution*
  Nodules confined to the centrilobular area are commonly seen in infectious airway disease, hypersensitivity pneumonitis, and respiratory bronchiolitis. They can appear as ground-glass opacity or show the *tree-in-bud* sign, visualized as an irregular branching structure expression of dilated and mucus-filled centrilobular bronchioles, usually indicating an infectious process involving the airways.
- *Perilymphatic distribution*
  Nodules are located in proximity of pleural surface, especially near fissures, and interlobular septa. Perilymphatic nodules are usually seen in sarcoidosis, several pneumoconioses, and lymphangitic spread.
- *Random distribution*
  Nodules not showing a prevalent distribution pattern, such in cases of metastases or miliary spread of granulomatous diseases.

The *high-attenuation pattern* can be represented by ground-glass opacity or consolidation on the basis of the partial or complete increase of lung density.

- *Ground-glass opacity*
  Ground-glass opacity can be the result of the alveolar filling by fluid, fibrosis, or cellular components, as well as of marked thickening of alveolar walls or surrounding interstitium: for these reasons, a ground-glass opacity is a rather unspecific finding, and its distribution can be a helpful feature to guide the differential diagnosis. Ground-glass opacity can be associated with a reticular pattern of septal thickening, forming the so-called crazy paving (i.e., in alveolar proteinosis). Areas with increased densities with lobular distribution alternated with non-affected areas are referred as *mosaic attenuation*: this finding is usually the expression of an obstruction of small airways, causing a compensatory oligemia with associated air trapping phenomena.
- *Consolidation*
  This condition is typically related to airspace diseases: acute consolidation can be seen in pneumonias, hemorrhage, or cardiogenic pulmonary edema, while chronic consolidation can be observed in chronic and organizing pneumonia or in conditions characterized by fibrotic evolution.

The *low-attenuation pattern* is the expression of fluid- or air-filled pulmonary lesions, including:

- *Cystic lung disease*
  Lung cysts are defined as radiolucent areas with <4 mm wall thickness (>4 mm are called cavities): they can be observed in lymphangioleiomyomatosis, Langerhans cell histiocytosis, and lymphocytic interstitial pneumonia.
- *Emphysema*
  It presents as areas of parenchymal destruction with diffuse low attenuation. It can be divided into *centrilobular emphysema*, the most common, strongly associated with cigarette smoke and with prevalence in upper lobes; *paraseptal emphysema*, next to fissures and pleural surfaces, frequently associated with bullae and spontaneous pneumothorax in young patients; and *panlobular emphysema*, affecting the whole secondary lobule, with prevalence in lower lobes, usually associated with deficiency of alpha-1-antitrypsin.

- *Bronchiectasis*
  They are represented by localized bronchial enlargement, with associated bronchial wall thickening and mucous filling of the bronchial lumen. The most frequent causes are recurring infections, chronic bronchitis, chronic obstructive pulmonary disease, and cystic fibrosis.

Key Learning Points

- CT is the most sensitive technique for the assessment of pulmonary parenchyma: it has a pivotal role in diagnosis, staging, and follow-up of pulmonary cancers.
- High-resolution CT can help in the evaluation diffuse lung disease, allowing an accurate analysis of pulmonary interstitium.
- CT can play a role in the evaluation of airways, and it can be used to guide interventional procedures, such as biopsies or drainages.
- Differential diagnosis and management of the solitary pulmonary nodule depend on several features, such as size, shape, composition, and contrast enhancement. Thus, it is crucial to establish imaging features that help the physicians to distinguish between benign and malignant nodule. The Fleischner Society periodically updates guidelines for the management of pulmonary nodules.
- CT interpretation of interstitial involvement requires a structured approach considering the dominant pattern (reticular, nodular, high attenuation, low attenuation), its location within the secondary lobule (i.e., centrilobular or perilymphatic), its distribution in the lung (upper vs lower lobe, central vs peripheral location), and the presence of additional findings such as pleural effusion or enlarged lymph nodes.

14.6 Mediastinum and Pleura

CT has a pivotal role in the evaluation of the mediastinum, and it is generally used for the evaluation of mediastinal masses and for lymph node staging of lung cancer. The pleura and thoracic wall can be assessed as well, even if the emerging role of MRI in entities such as malignant pleural mesothelioma is slowly changing the diagnostic work-up.

14.6.1 Differential Diagnosis of Mediastinal Masses

Mediastinal masses are relatively rare (about 3% of chest tumors), and they often represent an incidental finding on CT performed for different indications (especially lung cancer screening programs); however, they can cause clinical symptoms (i.e., cough, dyspnea, dysphagia, etc.) requiring detection and characterization. Standard CT protocols include one or two phases of contrast-enhanced images, while recent advances in technology feature low-dose protocols (especially for lung cancer screening), gated acquisitions for more reliable vascular evaluation, and dual-energy CT for better tissue characterization. The role of CT densitometry on non-enhanced images in the classification of mediastinal masses can be summarized in Table 14.3.

Table 14.3 Role of NECT and contrast enhancement in the classification of mediastinal masses

Role of NECT and contrast enhancement in the classification of mediastinal masses	
Fluid-containing (cystic) mediastinal masses	Cystic thymoma
	Cystic teratoma
	Pericardial cysts
	Bronchogenic/esophageal cysts
	Lymphangioma
	Cystic degeneration of several tumors
Fat-containing mediastinal masses	Lipoma
	Liposarcoma
	Thymolipoma
	Benign teratoma
	Diaphragmatic hernia
Calcium-containing mediastinal masses	Thyroid masses
	Thymic masses
	Germ cell tumors
	Treated lymphomas
	Lymph nodes (i.e., in tuberculosis, silicosis, sarcoidosis, etc.)
	Vascular pseudomasses
Enhancing mediastinal masses	Hyperenhancing lymph nodes
	Thyroid tissue
	Paragangliomas
	Hemangiomas
	Vascular etiologies

The crucial point in differential diagnosis of mediastinal masses is to distinguish between primary and secondary tumors, since the latter are more common and they are most frequently represented by lymphatic masses or metastases. Discrimination of pseudolesions such as congenital vascular variants may be challenging. In general, the evaluation and differential diagnosis of mediastinal masses is based on their location (anterior, middle, posterior, and superior compartment), but a more accurate classification based on CT axial images has been proposed by Fujimoto et al. (JART general rules).

The anterior mediastinum is most frequently involved (54%), and most of the *anterior mediastinal masses* are included in the "5Ts" (Table 14.4):

- *Thymic masses*
  Thymic hyperplasia can be detected in several pathologic conditions, and it is a frequent occurrence as a "rebound" phenomenon after stress or chemotherapy. Benign and

malignant thymomas represent a neoplastic proliferation of thymic epithelium: there are three main variants: benign *thymoma, invasive thymoma,* and *thymic carcinoma*. In consideration of the wide individual variability, it is difficult to estimate a "normal" size in patients <20 years old. In grown-up subjects, maximum transverse diameter should not exceed 15 mm. Benign thymomas present as well-defined round masses with soft tissue density located in the anterosuperior mediastinum. Features indicative of invasion of adjacent structures should raise the suspect of more aggressive lesions. *Thymic cysts* frequently develop following chemo- or radiotherapy, and they can show variable density values (from −15 to 80 HU) due to the common occurrence of intracystic bleeding.

- *Thyroid or parathyroid masses*
  They are mainly represented by intrathoracic goiter and thyroid tumors. See *Head and neck* section for a more detailed discussion on these topics.
- *Lymphomas*
  They are primary neoplastic lesions of the reticuloendothelial system, and they can be classified into *Hodgkin disease* (HD) and *non-Hodgkin lymphomas* (NHL). CT can be useful to determine disease extent, to assist therapeutic planning and to evaluate the response to treatment. HD has an insidious onset, spreading within contiguous lymph node groups. At CT examination HD may appear as a single enlarged lymph node or large conglomerated masses. Predominant thymic involvement is observed in 30% up to 70% of patients, usually associated with nodal enlargement in other mediastinal stations. These lesions are usually isodense compared to soft tissues, and they show only mild contrast enhancement. Calcifications are frequent only after treatment. NHL patients often present with advanced disease: tumor spread can involve extranodal structures and lung or pleural involvement can be seen.
- *Extragonadal germ cell tumors*
  They are frequently located within the thymic loggia and they frequently affect young men. *Dermoid cysts* are round capsulated masses with hydric or fatty density that may contain calcifications of ossification's foci. *Teratomas* may show variable density and malignant variants present ill-defined margins and wide necrotic areas; they can also dislocate mediastinal vascular structures. Other types of malignant germ cell tumors, such as seminomas, are rare and usually present as lobulated solid masses.
- *Thoracic aneurysm and vascular anomalies*
  Aortic aneurysms are represented by a permanent dilatation of the aortic wall. Ascending aorta is considered aneurysmatic when showing a cross-sectional diameter >4 cm (while the threshold is >3 cm in descending aorta). Abnormal wall dilatation can lead to rupture. The detection of aortic wall anomalies including intraluminal calcification can be a sign of acute aortic syndrome, which requires urgent diagnostic assessment and clinical follow-up.

Table 14.4 The "5Ts" of anterior mediastinal masses

Thymic masses (thymomas, thymolipomas, thymic carcinoma, thymic hyperplasia)
Thyroid or parathyroid masses (goiter, tumors)
(Terrible) Lymphomas (Hodgkin, non-Hodgkin)
Teratoma (especially in children)
Thoracic aneurysm and vascular anomalies

Middle mediastinal masses account for 20% of overall mediastinal masses and they include:

- *Lymphadenopathies*
  Lymph nodes are the most common site of metastatic spread, and their evaluation has both a prognostic and a therapeutic significance (i.e., operable vs non-operable disease, adjuvant/neoadjuvant radio-chemotherapy). Imaging findings include size, typically assessed with long- and short-axis diameters (Fig. 14.9), morphology, homogeneity, conspicuity, and clustering. Regarding size,

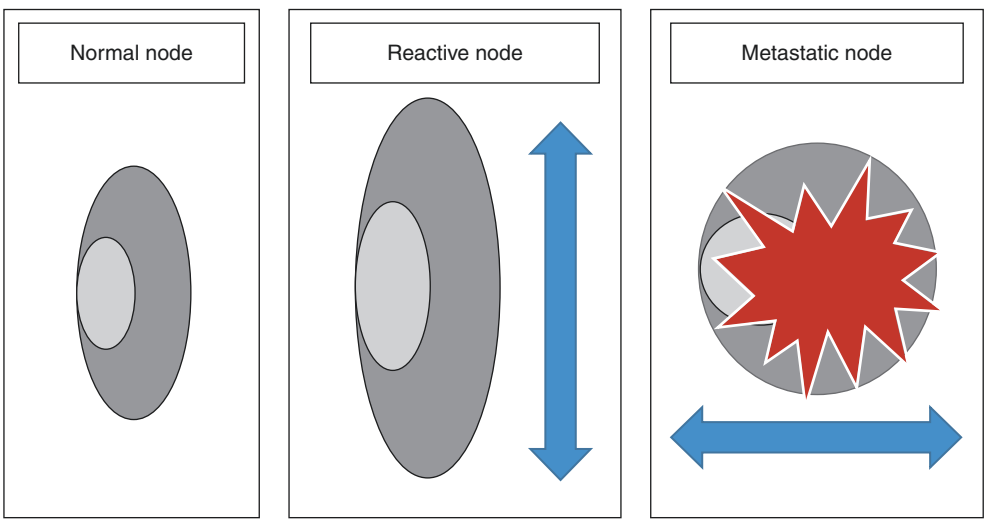

Fig. 14.9 Schematic summary of size and morphology changes in reactive lymph nodes, with increase of long-axis diameter, and metastatic lymph nodes, with increase of short-axis diameter and rounding of nodal shape

normal mediastinal lymph nodes should not exceed 10 mm in short transverse diameter, with the exception of subcarinal nodes, considered normal up to 15 mm; however, though accepted and routinely used in RECIST criteria, this threshold is debated and far from perfect in terms of sensitivity and specificity. Other findings that should alert the reader when evaluating lymph nodes are inhomogeneity (often due to necrosis), strong enhancement (often associated with hypervascular primary tumors), and changes in size of morphology, such as the presence of spiculated borders. Location (ipsi- vs contralateral) and clustering have to be considered as well in the diagnostic evaluation, since clustered nodes are suspicious besides their effective enlargement.

- *Congenital mediastinal cysts*
  They include bronchogenic and enteric cysts, foregut duplication cysts, and pericardial cysts; they are often an incidental finding in adult asymptomatic patients. *Bronchogenic cysts* are located close to the tracheobronchial tree, and their CT features include the presence of a well-defined non-enhancing oval mass, with a thin wall that can present contrast enhancement. They are characterized by a homogeneous fluid density, and they typically show a paratracheal or carinal location. *Esophageal duplication cysts* are difficult to distinguish from bronchogenic cysts due to their similar embryonic origin. They are more frequently located in posterior mediastinum, next to or inside the distal thoracic esophagus, although they usually do not communicate with the esophageal lumen. *Pericardial cysts* originate from the pericardium, but they rarely communicate with the pericardial cavity. They are most frequently located in the right cardiophrenic angle, and they usually present a water density with well-defined margins and spherical or triangular shape.
- *Vascular anomalies and malformations*

Differential diagnoses of *posterior mediastinal masses* (about 26% of total) include:

- *Neurogenic tumors*
  They can be divided into *nerve sheath tumors*, such as schwannomas or neurofibromas, and *neuroblastic tumors*, such as malignant neuroblastoma and benign ganglioneuroma. The first ones are elliptical paravertebral masses with mild contrast enhancement that may enlarge intervertebral foramens. Ganglion cell tumors are rare, show intense contrast enhancement, and are frequently located next to the aortic arch or posterior pericardium.
- *Foregut duplication cysts* (see middle mediastinal masses)
- *Lymphomas* (see anterior mediastinal masses)
- *Lymphadenopathies* (see middle mediastinal masses)
- *Extramedullary hematopoiesis*
  In patients with thalassemia or sickle cell anemia, hyperplasia of hematopoietic tissue can produce large paravertebral masses with soft tissue density and convex margins, extending caudally along distal thoracic spine but without bone erosion phenomena. This condition is frequently associated with splenomegaly.

14.6.2 Pleural and Chest Wall Tumors

Chest wall tumors are mainly metastatic, usually from adenocarcinomas, or can be caused by the spread of a peripheral bronchogenic carcinoma. They appear as masses located in the muscular layers obliterating fat planes, and they are usually evident only in post-contrast acquisition. The implant area and the width of connection angles may indicate the origin of the lesion (Fig. 14.10).

Malignant pleural mesothelioma is highly correlated with asbestos exposure, with a long latency period (up to 30 years). CT accurately depicts advanced tumors, while is less reliable in early lesions. Mesothelioma may develop as large plaques or as irregular nodular thickenings of the pleura, with heterogeneous enhancement after contrast media. Pleural effusion and pulmonary entrapment may be seen, while some lesions present with pericardial effusion, erosion of ribs, contralateral pleural involvement, and intrapulmonary metastasis.

14.6.3 Nonneoplastic Pleural Diseases

Inflammatory and post-traumatic pleural involvement is quite frequent in routine clinical practice. The most common entity is *pleural effusion* (Fig. 14.11): it may consist of serous, lymphatic, or hemorrhagic (with higher density values) components. CT can reveal even small amounts of effusion (>15 mL), and the fluid usually layers in posterobasal regions, while organized effusions may be found anywhere in the pleural cavity. Pleural empyema may be the consequence of a purulent effusion: CT shows marked con-

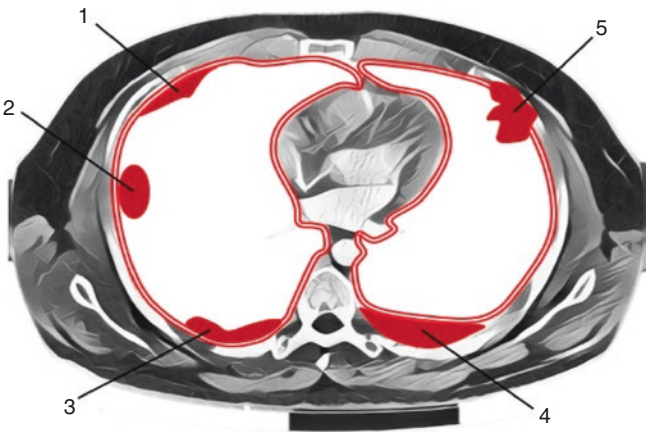

Fig. 14.10 Schematic summary of pleural, extrapleural, and pulmonary lesions and differential diagnosis based on the implant area and width of connection angles. Pleural lesion (1), pulmonary lesion (2), pleural effusion (3), extrapleural lesion (4), intrapulmonary lesion with pleural and chest wall involvement (5)

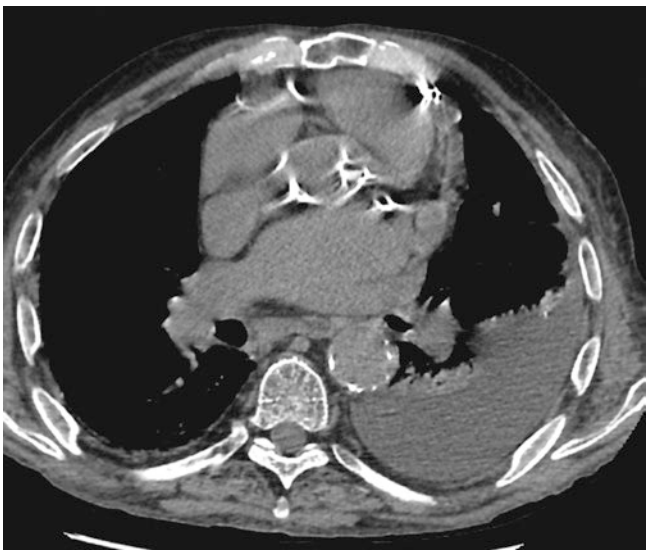

Fig. 14.11 An 83-year-old patient with persistent left pleural effusion and atelectasis of adjacent lung parenchyma

trast enhancement and thickening of pleural sheets surrounding the effusion (*split pleura sign*). *Pneumothorax* can be outlined at CT by direct visualization of the pleural sheets separated by a gas collection.

Key Learning Points

- CT has a pivotal role in the evaluation of the mediastinum, and it is generally used for the evaluation of mediastinal masses and for lymph node staging of lung cancer.
- Mediastinal masses are relatively rare (3% of chest tumors), and they often represent an incidental finding on CT performed for different reasons; however, they can cause clinical symptoms (i.e., cough, dyspnea, dysphagia, etc.) requiring diagnostic work-up and characterization.
- The crucial point in differential diagnosis of mediastinal masses is to distinguish between primary and secondary tumors, since the latter are more common and they are most frequently represented by lymphatic masses or metastases.
- A conventional approach to mediastinal mass evaluation and differential diagnosis is based on their location.
- Chest wall tumors are mainly metastatic, usually from adenocarcinomas, or can be caused by the spread of a peripheral bronchogenic carcinoma.
- Inflammatory and post-traumatic pleural involvement, such as in case of pleural effusion or pneumothorax, is quite frequent in routine clinical practice.

14.7 Abdomen and Pelvis

CECT is a fundamental tool for the characterization of lesions initially detected with other diagnostic exams (e.g., ultrasound), for diagnosis in emergency situations, and for staging and follow-up of oncologic patients. CECT allows for detection of pathological findings that provide a probabilistic diagnosis based on the contrast enhancement pattern of the lesions in the dynamic phase. The lesions most commonly encountered during a body CECT exam are discussed below.

14.8 Liver

Liver lesions can be categorized into benign and malignant lesions (primary and secondary). Flow charts to guide in the CT differential diagnosis of liver lesions is provided in Tables 14.5 and 14.6.

14.8.1 Benign Lesions

Liver cysts are the most common liver lesions, and they can be solitary or multiple. On NECT, cysts have a watery density (0–15 HU). Simple cysts do not show contrast enhancement after contact media injection. When multiple cysts with different size involve the kidney as well, autosomal dominant polycystic kidney disease (ADPKD) should be considered in the differential diagnosis.

Liver hemangiomas are benign vascular malformations, and they are the second most common incidental finding that can be detected in asymptomatic patients. Considering their frequent occurrence during radiological examinations (especially with ultrasound), the differential diagnosis with malignant hepatic lesions is of crucial relevance, especially in those patients who have a history of neoplasia. Liver hemangiomas can be mainly divided into cavernous hemangiomas and in flash-filling hemangiomas that usually cannot be detected on NECT. Large cavernous hemangiomas typically show early peripheral contrast enhancement in arterial phase with a globular pattern and a progressive centripetal filling in portal and equilibrium phases (Fig. 14.12). The globular pattern implies the presence of a discontinuous and nodular peripheral contrast enhancement that progressively fills the lesion. Some malignant lesions like intrahepatic cholangiocarcinoma can have peripheral pattern of contrast enhancement in arterial phase with progressive fill, but without the nodular or globular pattern.

Lesions with complete arterial contrast enhancement and blood pool pattern on portal and equilibrium phase could be characterized as *capillary hemangiomas*. The blood pool pattern can be observed when a liver lesion has the same density of the portal veins on all dynamic phases. When present, blood pool is an important finding that suggests the diagnosis

Table 14.5 Flow chart of the differential diagnosis of hypervascular liver lesions

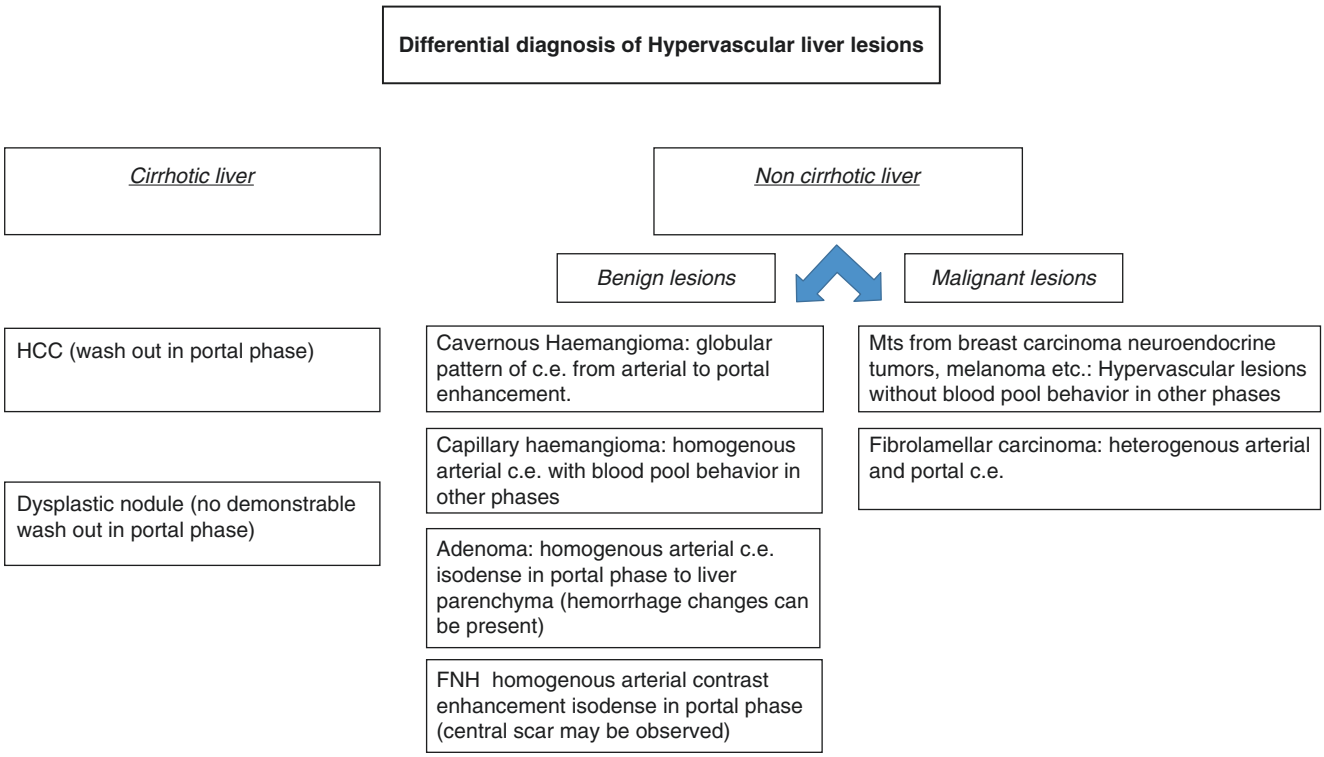

HCC hepatocellular carcinoma, *c.e.* contrast enhancement, *FNH* focal nodular hyperplasia, *Mts* metastases

Table 14.6 Flow chart of the differential diagnosis of hypovascular liver lesions

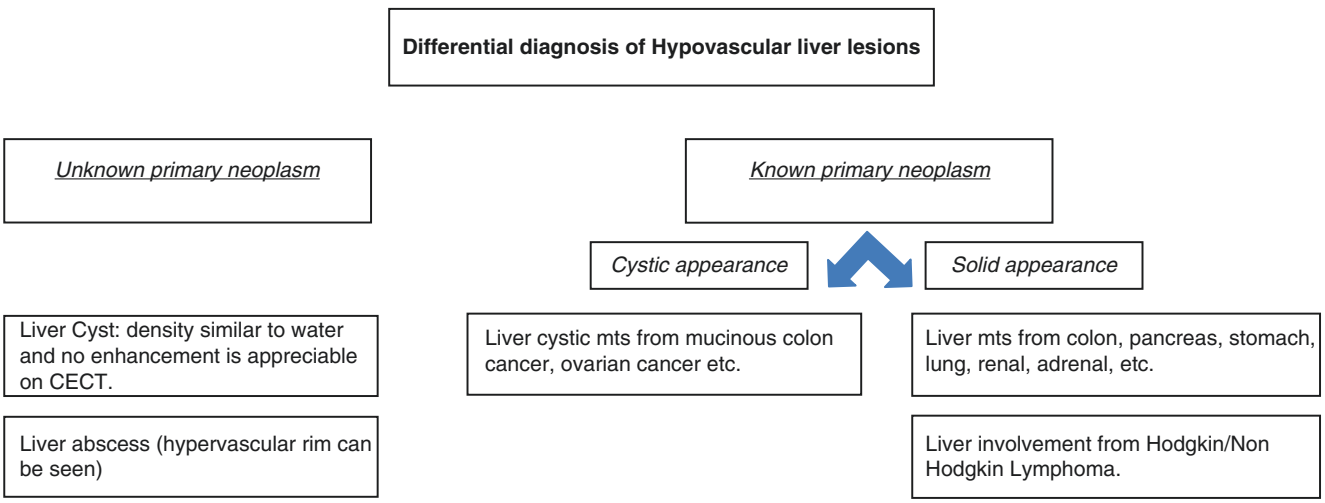

Mts metastases

of hemangioma. Capillary hemangiomas differ from transient hepatic attenuating difference (THAD) and from other lesions that exhibit hyper-attenuation only in the arterial phase due to the presence of blood pool behavior. THAD is secondary to perfusion alterations in the liver parenchyma that may occur isolated or in association with other liver pathologies. These pseudolesions are appreciated only on arterial phase, and they become isodense compared to the surrounding liver parenchyma in the other CT phases.

Focal nodular hyperplasia (FNH) is a solitary regenerative hepatic lesion characterized by a localized anomaly of the biliary draining system. It typically presents as a mass with sharp margins, and it can be supplied by a hepatic artery with a dedicated hepatic venous drainage system. Focal nod-

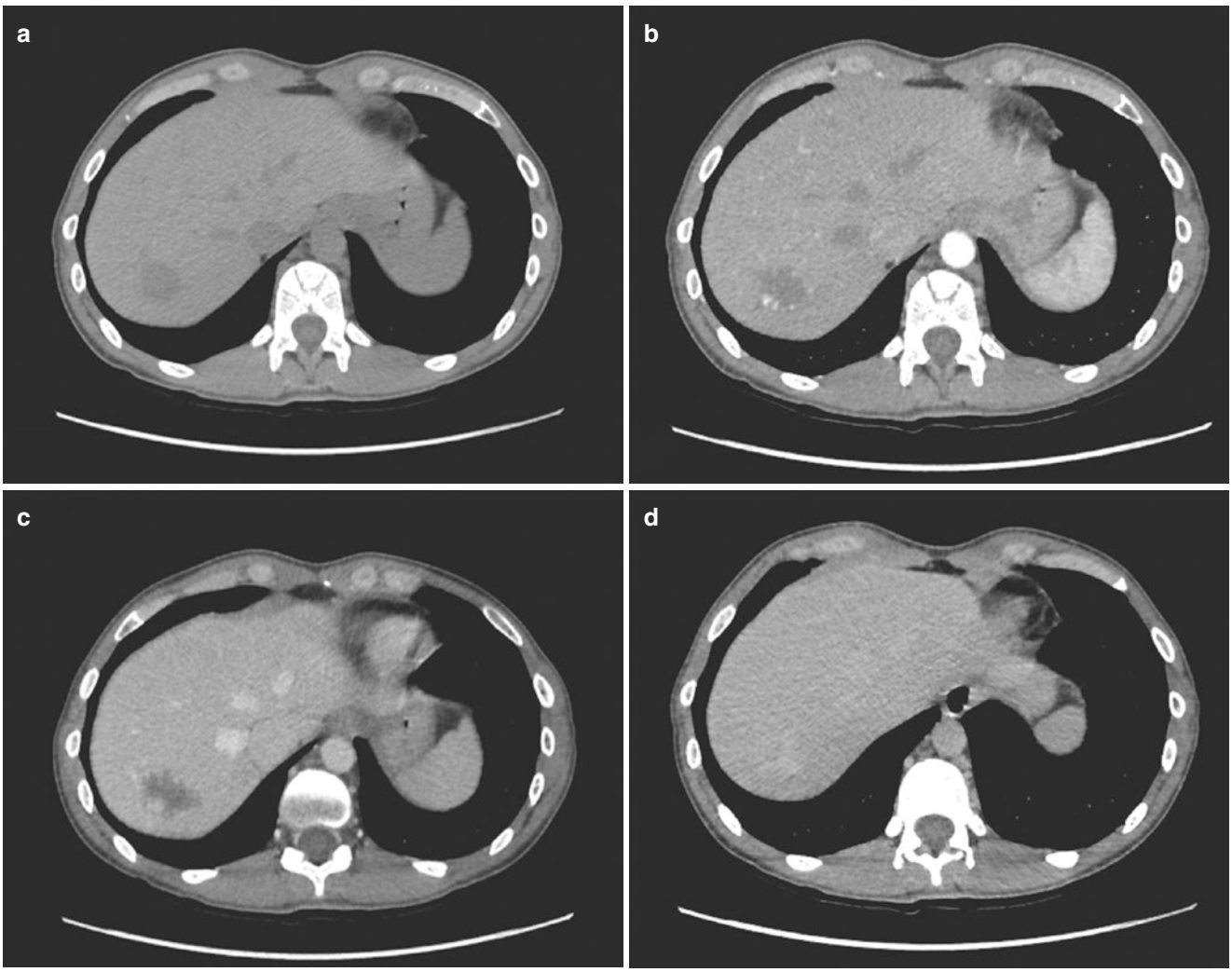

Fig. 14.12 Liver hemangioma. NECT (**a**) shows a hypo-attenuating lesion in the right liver lobe. A globular pattern of contrast enhancement with centripetal filling can be observed on arterial (**b**) and portal phase (**c**). Equilibrium phase (**d**) shows a complete enhancement of the lesion

ular hyperplasia is the second most common benign solid hepatic lesion, and it is found especially in young and middle-aged women. The typical behavior of FNH on CECT is bright homogenous complete arterial contrast enhancement without washout phenomena (Fig. 14.13). During the portal and equilibrium phases, the lesion becomes isodense to the liver parenchyma. In 30% of cases, FNH has a central scar that is hypo-attenuating on NECT and arterial and portal phase and shows contrast enhancement in the equilibrium phase. FNH is considered atypical when central scar and/or a central artery can't be observed. When the features of a hypervascular liver lesion are not completely suggestive of a FNH, especially in woman with a prior history of breast cancer (breast metastasis may also appear hyper-attenuating on arterial phase), further examinations such as magnetic resonance imaging must be considered.

Hepatic adenomas are uncommon benign liver lesions usually encountered in young and middle-aged women that have been on oral contraceptives for a long time. These lesions are usually solitary and may frequently show hemorrhagic phenomena. Hepatic adenomas have a right lobe predilection in subcapsular location, and they usually present with well-defined margins. The attenuation of hepatic adenomas on NECT depends on the presence of fat tissue that makes the lesion hypo-attenuating. Hemorrhagic phenomena can give the lesion a hyper-attenuating appearance, compared to liver parenchyma. On CECT, hepatic adenomas present a strong arterial contrast enhancement, and a pseudocapsule can be frequently seen. The enhancement in adenomas typically does not persist due to the presence of arteriovenous shunting.

Liver abscesses are localized fluid collections containing necrotic and purulent material. Liver abscesses may have different causes: in developing countries, the parasitic cause is the most common, mainly represented by protozoan and helminthic diseases such as echinococcosis and amebiasis, while in

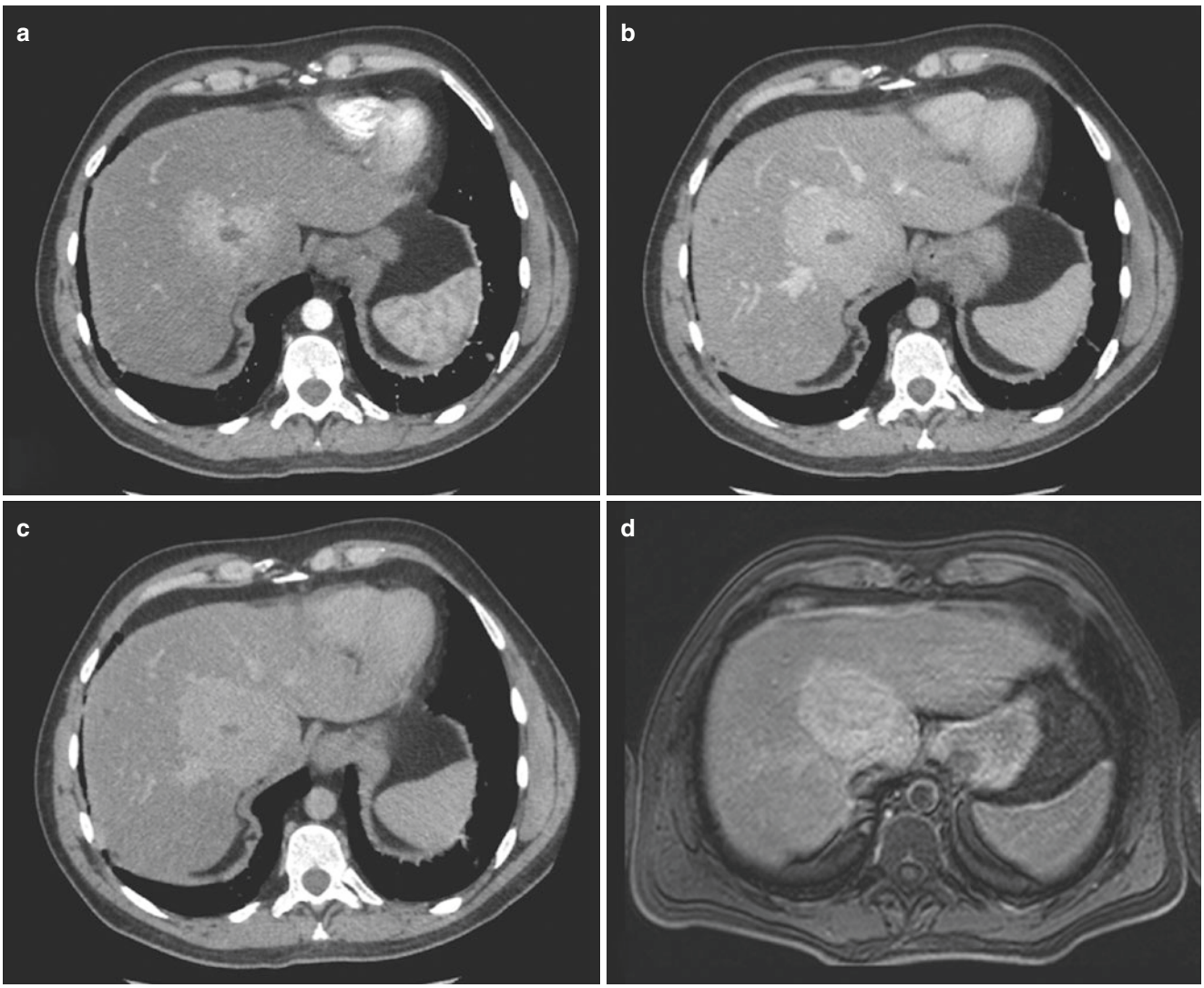

Fig. 14.13 Liver FNH. Arterial phase (**a**) shows a round lesion with rapid contrast enhancement, and a central scar can be observed. The lesion is hyper-attenuating compared to the liver parenchyma on portal (**b**) and equilibrium phase (**c**). MR image acquired after 120 min after the administrarion of hepatospecific contrast material (**d**) showing hyperintensity of the lesion compared to liver parenchyma that is highly suggestive of FNH

western countries, the most frequent etiology is bacterial, and it occurs as comorbidity in immunocompromised patients, in abdominal sepsis, and in necrotizing enterocolitis. Amebic abscess is usually solitary, whereas fungal and bacterial liver abscesses are multiple. Liver abscesses do not have a typical pattern on NECT and CECT. Lesions are usually round with central hypo-attenuation with respect to the liver parenchyma in portal phase. A slightly hyper-attenuating peripheral rim can be observed on NECT, showing contrast enhancement in arterial and portal phase. Sometimes a central hypo-attenuating area can be observed (fluid collection due to necrotic changes), surrounded by an inner rim of hyper-attenuation that shows strong contrast enhancement on the arterial phase and an outer rim (due to liver parenchymal edema) that enhances on portal and equilibrium phases (the so-called *double target sign*).

14.8.2 Malignant Lesions

- *Primary liver lesions*

Hepatocellular carcinoma (HCC) is the most common primary hepatic tumor, usually associated with hepatic cirrhosis. The incidence of this lesion is strictly correlated to chronic HBV or HCV infection, especially in developing countries, and to alcohol abuse that lead to hepatic cirrhosis in western countries. Biliary atresia, biliary cirrhosis, food toxins (such as aflatoxin), and inborn metabolism failures (hemochromatosis, Wilson disease, and alpha-1-antitrypsin deficiency) are also important risk factors. HCC usually develops in a cirrhotic liver and can present as a solitary, large mass with well-defined margins or multiple, with

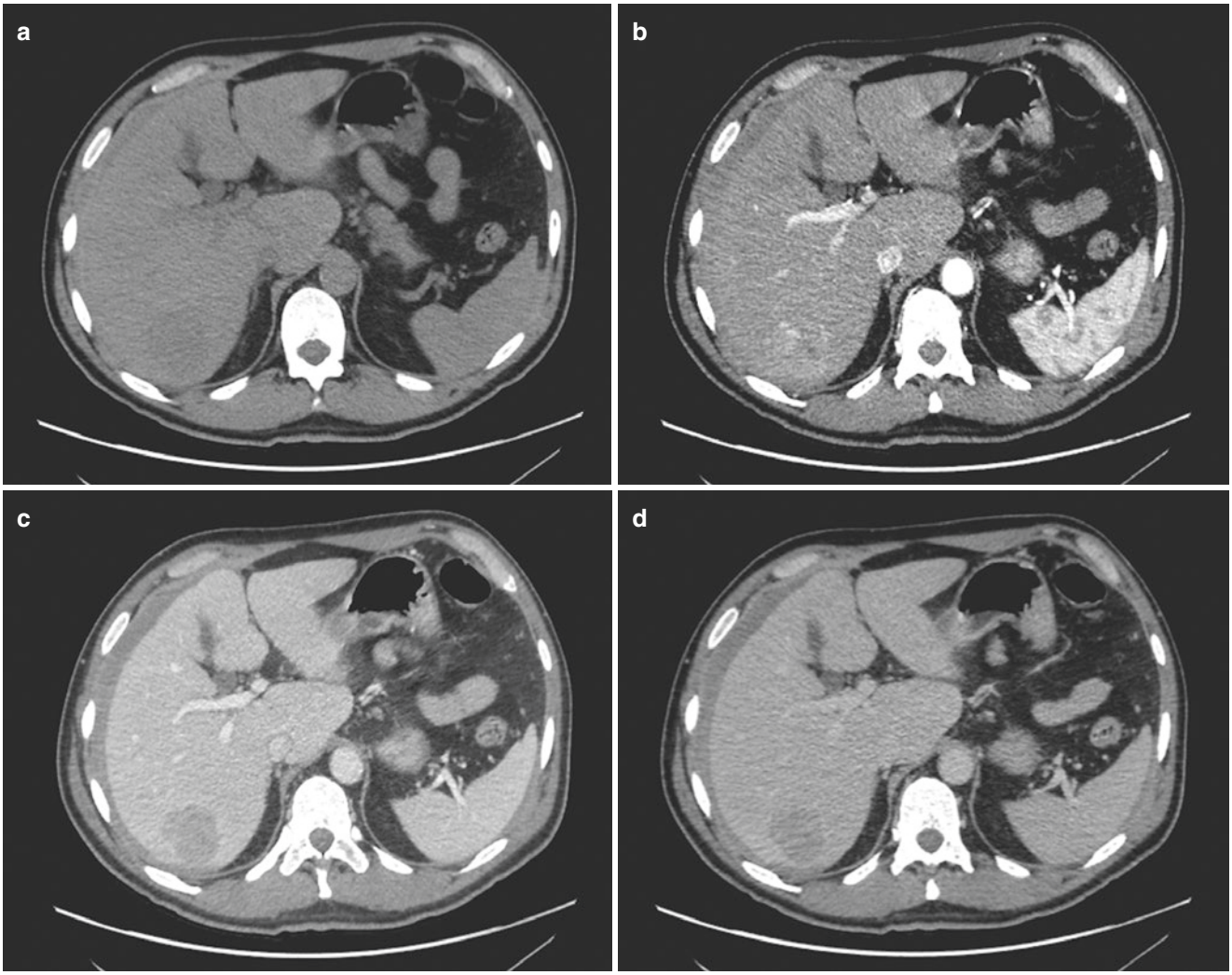

Fig. 14.14 Hepatocellular carcinoma (HCC). NECT phase (**a**): right liver lobe hypo-attenuating lesion. On arterial phase (**b**), the lesion shows a strong contrast enhancement that fills the lesion. On portal (**c**) and equilibrium phase (**d**), a washout phenomenon is demonstrable

variable attenuation. Another possible presentation is the infiltrative or diffuse type. In the latter case, the presence of nodular alterations of the parenchyma as regenerative nodules or dysplastic nodules may make the diagnosis of HCC more difficult. The typical HCC pattern of contrast enhancement consists in a hyper-attenuation in arterial phase due to branch of hepatic artery vascularization supply. The pathognomonic sign of HCC is the early contrast enhancement with washout phenomena in portal and equilibrium phases (Fig. 14.14). When an early hyper-attenuation on arterial phase is seen into a regenerative nodule, a small HCC with "nodule in nodule" appearance must be suspected. Nodular HCC presents in more than half of the cases (50–80%) with a peripheral pseudocapsule. Furthermore, HCCs may infiltrate the portal vein causing thrombosis and portal hypertension. In this case a cavernous transformation of the portal vein can be observed (tortuous venous channel that replace the portal vein). Other liver lesions like portosystemic venous shunts, THAD, focal fatty changes, or skip areas in fatty liver may be observed.

Dysplastic nodules enter in the differential diagnosis with HCC nodules. On CECT they often exhibit early contrast enhancement on the arterial phase, but, unlike HCC nodules, they do not show washout phenomena.

Regenerative nodules are liver lesions observed in liver cirrhosis and are classified according to their size as micronodules, macronodules, and giant nodules. Nodules are characterized by the presence of a regular parenchymal architecture in which a certain amount of fibrotic tissue or iron deposits may be included. These findings are responsible for the modest hyper-attenuation on NECT. There is no difference in attenuation of regenerative nodules with respect to liver parenchyma on CECT study.

Fibrolamellar carcinoma is a variant of HCC that occurs in younger patients with no correlation with common HCC risk factors. This type of tumor is a well-circumscribed

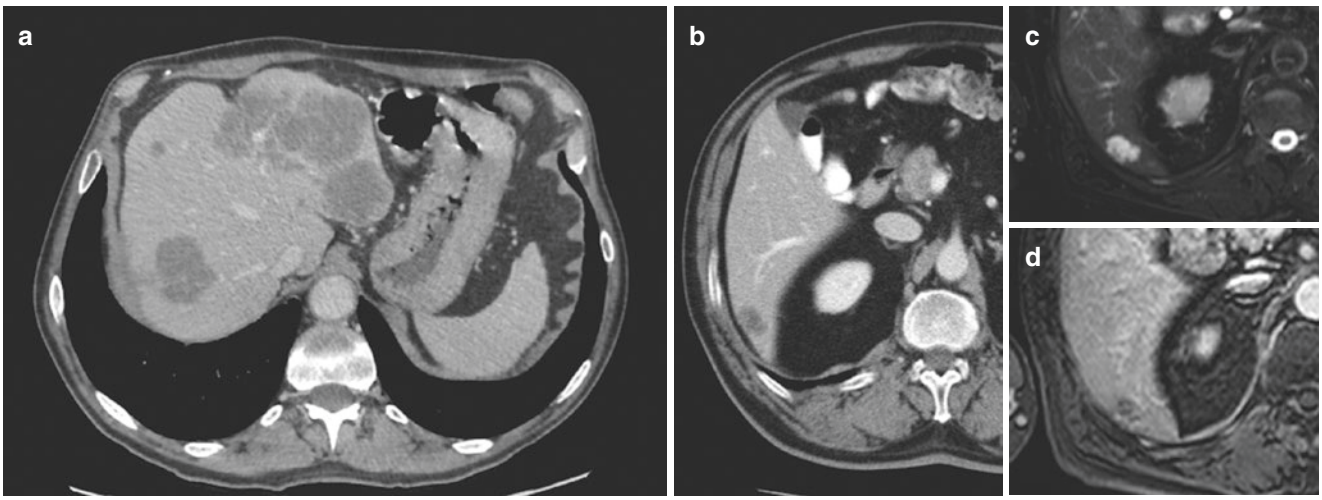

Fig. 14.15 CECT on portal phase (**a**) shows many round hypovascular lesions that are suggestive for metastases (the patient has a prior history of colonic neoplasm). A small hypovascular lesion on VI liver segment can be identified (**b**). Thin intra-lesion septa are present. The patient's history of mucinous colonic tumor requires further investigation with MRI. The cystic nature of the lesion is confirmed by the T2 fat saturation MRI (**c**), and the thin septa can be observed on 3D T1 fat saturation MRI (**d**)

lesion with sharp margins, and it contains a portion of fibrotic tissue organized in lamellar bands usually forming a central scar. On NECT a central area of low density due to necrosis or fibrosis can be seen. Calcifications can be observed in central scar in up to 30% of all cases. Fibrolamellar carcinomas commonly are heterogeneously hypervascular lesions in arterial and portal phases.

- *Secondary liver lesions*

Liver metastases are the most common malignant liver lesions in an non-cirrhotic liver, and in most cases they are not appreciable on NECT. Metastases on CECT study can be hypervascular (most commonly from renal cell carcinoma, breast carcinoma, islet cell tumor, melanoma and sarcoma, pheochromocytoma, carcinoid and thyroid carcinoma) or hypovascular (most commonly from the GI tract, breast, pancreas, lung, and cervix) (Fig. 14.15). In the detection of small liver metastases, arterial phase is useful in both types of lesions: in hypovascular metastases, it can accurately demonstrate the peripheral rim, and in hypervascular metastases, it shows heterogeneous hyper-attenuation (this type of metastasis are likely isodense to liver parenchyma in the portal phase). The portal and equilibrium phases are the most important phases in detection of hypovascular metastases that typically show hypo-attenuation compared to normal liver parenchyma. NECT is helpful to distinguish calcified metastases from the colon mucinous tumor, stomach, adnexa, breast, thyroid, lung or kidney, carcinoid, and melanoma. When the patient has concomitant fatty liver disease, liver metastases may appear iso- or slight hyper-attenuating with respect to the liver parenchyma in portal phase.

Key Learning Points

- Liver lesions can be categorized in benign and malignant lesions, and malignant lesions can be divided into primary and secondary.
- Liver cysts are the most common liver lesions and they can be solitary or multiple.
- Liver hemangiomas are benign vascular malformations, and they are the second most common incidental finding that can be detected in asymptomatic patients.
- Focal nodular hyperplasia and hepatic adenomas are uncommon benign liver lesions usually encountered in young and middle-aged women.
- Hepatocellular carcinoma (HCC) is the most common primary hepatic tumor, usually associated with hepatic cirrhosis. The typical HCC pattern of contrast enhancement consists in a hyper-attenuation in arterial phase due to branch of hepatic artery vascularization supply. The pathognomonic sign of HCC is the early contrast enhancement with washout phenomena in portal and equilibrium phases.
- Liver metastases are the most common malignant lesions in non-cirrhotic liver; on CECT study they can present hypervascular (most commonly from renal cell carcinoma, breast carcinoma, islet cell tumor, melanoma and sarcoma, pheochromocytoma, carcinoid, and thyroid carcinoma) or hypovascular behavior (most commonly from the GI tract, breast, pancreas, lung, and cervix).

14.9 Biliary Tree

Biliary lesions affect the gallbladder and both intrahepatic and extrahepatic bile ducts. They can be benign or malignant.

Gallbladder carcinoma is usually asymptomatic at the time of the diagnosis, and it is often an incidental finding during an abdominal ultrasound or a CT exam performed for other reasons. Long-standing gall bladder stones are the major risk factor for the development of this condition. Others risk factors include chronic cholecystitis, familial adenomatous polyposis syndrome, gall bladder polyps (when >10 mm), porcelain gallbladder, and inflammatory bowel diseases. Gallbladder carcinoma is most frequent in elderly women. Clinical presentation can be different depending on the location of the tumor: if the lesion affects the fundus of the gallbladder, the tumor can infiltrate the adjacent liver parenchyma or the colon, and the first symptom could be the upper abdominal quadrant pain; if the lesion affects the gallbladder infundibulum, the initial symptom can be jaundice. On NECT, calcifications of gallbladder's walls could be present; when the wall is completely calcified and retracted, the gallbladder is called porcelain gallbladder. On CECT, gallbladder carcinoma can be seen as a solid polypoid mass with a diameter >10 mm, with diffuse wall thickening showing hyper-attenuating pattern of contrast enhancement, or as solid tissue that completely replaces the gallbladder. The latter is the most frequent presentation: it appears as an infiltrating heterogeneous mass with slightly and patchy contrast enhancement in arterial and portal phases. Dilatation of intrahepatic biliary ducts, lymphadenopathies, and ascites may be present as features of advanced disease.

Cholangiocarcinoma is the second most frequent malignant hepatic tumor and it originates from cholangiocytes. The main risk factors for the development of cholangiocarcinoma are primary sclerosing cholangitis (PSC, especially in western countries), recurrent pyogenic cholangitis, choledocholithiasis, and *Clonorchis sinensis* infection in Asian countries. Cholangiocarcinomas can arise from intrahepatic bile ducts or extrahepatic bile duct epithelium. The intrahepatic form is divided into a peripheral type that is usually a hypodense mass on NECT with associated intrahepatic bile duct dilatation (capsular retraction is often seen) and a central (hilar) type that is a mass at the level of hepatic duct confluence. Cholangiocarcinoma is considered peripheral if it originates peripherally from a secondary branch of a biliary hepatic duct and hilar when it originates from a biliary hepatic duct or common hepatic duct (Klatskin tumor). Cholangiocarcinomas may be classified also depending on the shape and biological behavior. It may be mass forming, infiltrating, periductal, or intraductal. The extrahepatic type of cholangiocarcinoma is typically infiltrative in association with common bile duct and intrahepatic bile ducts dilatation. A mass-forming cholangiocarcinoma on CECT typically shows early complete rim enhancement with progressive, centripetal non-globular pattern of enhancement in portal and equilibrium phase (Fig. 14.16). Invasion of portal veins is not a rare occurrence, especially in hilar type. Infiltrative periductal cholangiocarcinoma is most common at hepatic hilum, and it is often associated with narrowing or dilatation of peripheral bile ducts due to pathological thickening of periductal hepatic parenchyma. The intraductal infiltrative cholangiocarcinoma may show the presence of polypoid lesion into a duct that demonstrates contrast enhancement on portal phase compared to NECT.

Key Learning Points

- Biliary lesions affect the gallbladder and both intrahepatic and extrahepatic bile ducts. They can be benign or malignant.
- Cholangiocarcinoma is the second most frequent malignant hepatic tumor, and can arise from intrahepatic or extrahepatic bile duct epithelium.
- Cholangiocarcinomas may be classified depending on the shape and biological behavior. It may be mass forming, infiltrating, periductal, or intraductal.

14.10 Pancreas

Lesions in the pancreas can be divided into solid and cystic as summarized in Table 14.7).

14.10.1 Pancreatic Cystic Tumors

Pancreatic cystic tumors show fluid density on NECT. The lesions can be divided into *intraductal papillary mucinous neoplasm* (IPMN), *mucinous pancreatic cystadenomas*, and *pancreatic serous cystadenoma*.

There are three types of IPMN: secondary branch type, main duct type, and mixed type. The secondary branch type with a multicystic appearance is most likely due to a dilatation of secondary pancreatic ducts (usually at the level of pancreatic head). MR cholangiography is able to demonstrate a communication between the multicystic lesions and the main pancreatic duct. The isolated main duct type of IPMN consists of a dilatation of the main pancreatic duct of <5 mm. Mucous material with fluid-density values may fill the duct even at the level of the Vater papilla, which bulges

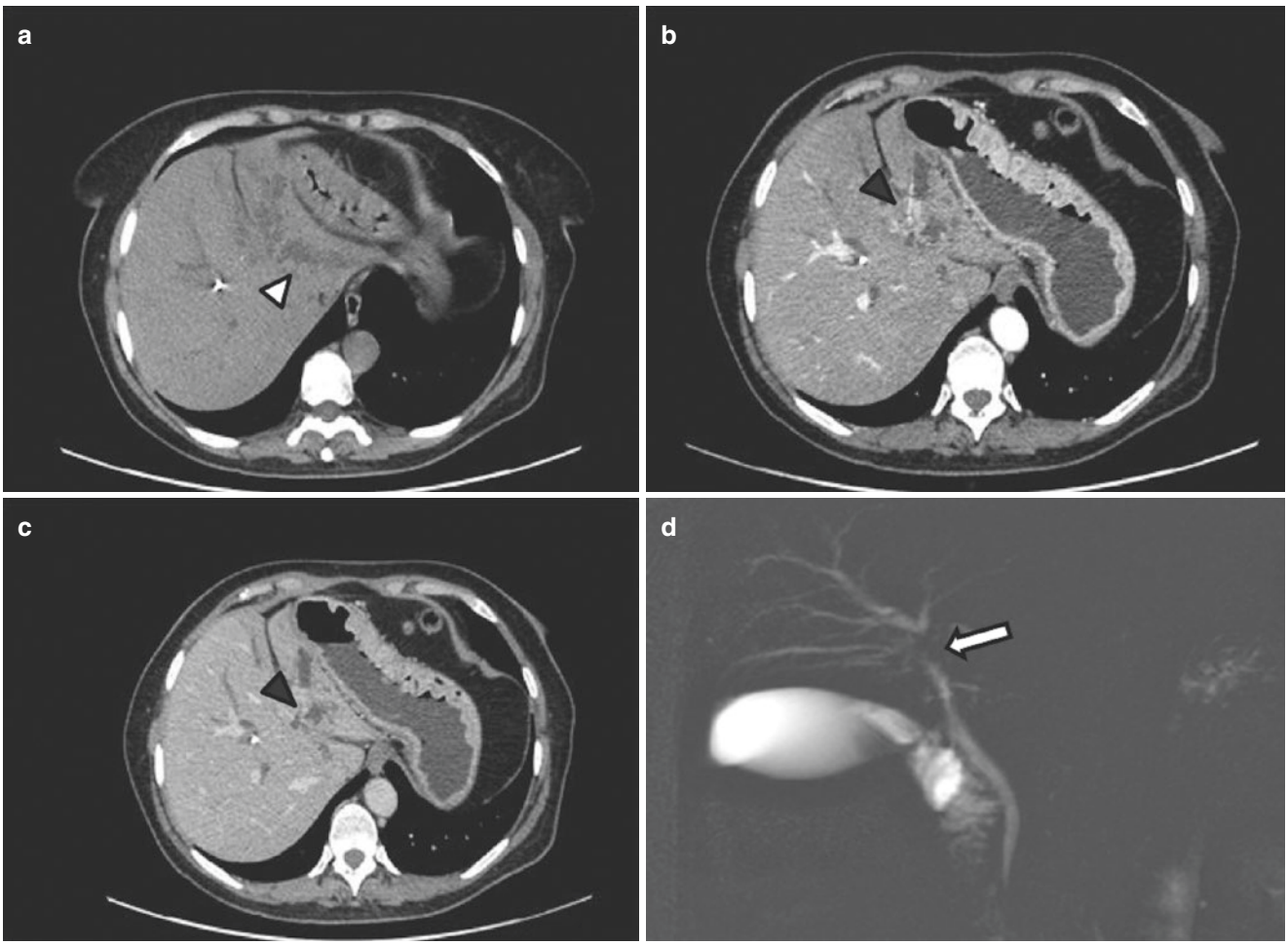

Fig. 14.16 Intrahepatic liver CCC. NECT image (**a**): the biliary drainage system of the left liver lobe (II segment mainly) and of IVa segment is dilated (white arrowhead). CECT on arterial phase (**b**) shows a peripheral contrast enhancement that fills the lesion (black arrowhead). The lesion is filled by contrast without a globular pattern on portal phase (**c**). MRI cholangiography (**d**) easily demonstrates the biliary obstruction at the level of left biliary duct bifurcation (white arrow)

Table 14.7 Flow chart of the differential diagnosis of pancreatic lesions

Differential diagnosis of pancreatic lesions

Cystic lesion	*Solid lesion*	
	Hypervascular	*Hypovascular*
PSC: multiple small cyst in head of pancreas	Neuroendocrine tumor: body or tail with arterial contrast enhancement	Pancreatic adenocarcinoma: more likely in pancreatic head. Double duct sign
MPC: Large unilocular or multilocular in body of pancreas		Pancreatic metastasis from GI cancer, etc.
IPMN primary duct, secondary branch or mixed. When papillary projection present high suspicious of malignancy		

PSC pancreatic serous cystadenoma, *MCP* mucinous pancreatic cystadenoma, *IPMN* intraductal papillary mucinous neoplasm, *GI* gastrointestinal

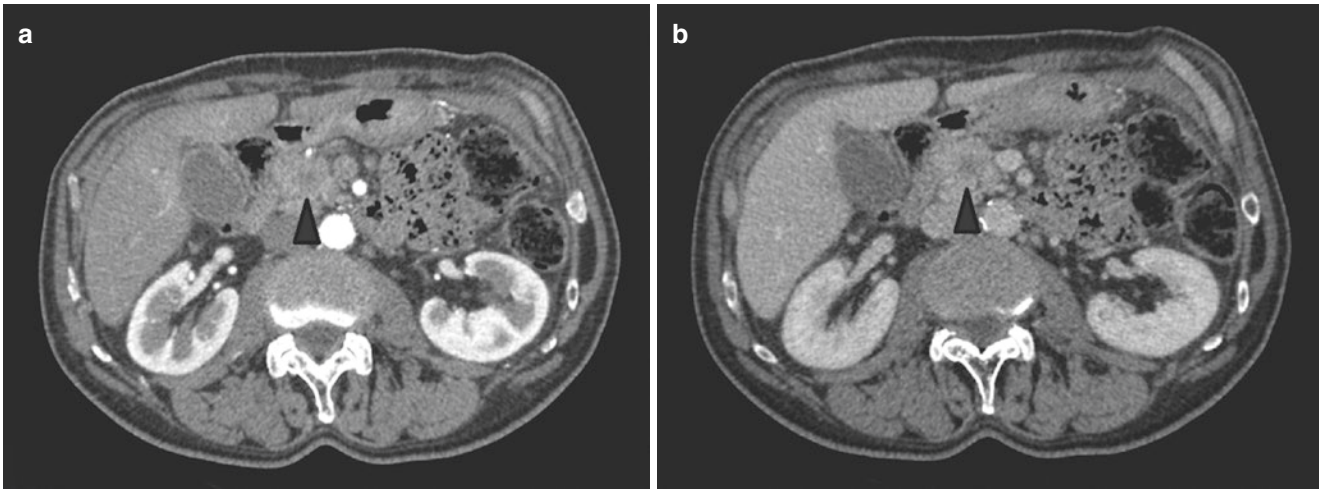

Fig. 14.17 Pancreatic adenocarcinoma. CECT on arterial phase (**a**): a hypovascular lesion is demonstrable on the head of the pancreas (arrowhead). The hypo-attenuating lesion persists on portal phase (**b**)

into the duodenum. The surrounding pancreatic parenchyma may be thinned due to atrophy. In the combined type, both primary ducts and the main duct are enlarged. Any papillary projection into a pancreatic duct with contrast enhancement on CECT is suspect for malignant transformation.

Pancreatic serous cystadenoma has a strong female predilection in elderly age. On CECT multiple (>6) small cysts (<2 cm) with thin wall are observed, usually in the pancreatic head. Calcification with central scar can be seen. *Pancreatic serous cystadenoma* is considered a benign lesion.

Mucinous pancreatic cystadenoma has a strong predilection for middle-aged women: the typical presentation is a large unilocular or multilocular cystic lesion (2–12 cm) most frequently observed in the body or tail of the pancreas. In this type of lesion, a communication with the main pancreatic duct should not be visible at MR cholangiography. *Mucinous pancreatic cystadenoma* is considered a premalignant lesion, and any papillary projection with contrast enhancement is suspicious for malignant transformation (mucinous pancreatic cystadenocarcinoma).

14.10.2 Pancreas Solid Neoplasms

Pancreatic ductal adenocarcinoma is a malignant neoplasm commonly affecting the elderly. The typical locations of pancreatic ductal adenocarcinoma are the head of the pancreas or the uncinate process. Pancreatic ductal adenocarcinoma commonly appears like an isodense mass on NECT and as a lesion with heterogeneous poor contrast enhancement in particular in arterial phase on CECT, probably due to the presence of fibrous tissue. A desmoplastic reaction can be usually observed around the lesion (Fig. 14.17). When the head of the pancreas is involved, a "double duct sign" (dilatation of main pancreatic duct and common biliary duct) can be observed, and particular attention should be paid to the presence of eventual vascular infiltration.

Endocrine tumors of the pancreas or pancreatic islet cell tumors are usually solitary, but they can be associated with MEN I, von Hippel-Lindau, or tuberous sclerosis. *Pancreatic islet cell tumors* can be classified in functional and nonfunctional or syndromic and non-syndromic, depending on whether or not they produce hormones. Another classification is based on the type of cells that constitute the tumor: glucagonoma, insulinoma, somatostatinoma, gastrinoma, and VIPoma. *Pancreatic islet cell tumors* can appear small or large in size. When small in size, they usually show sharp margins, sometimes with calcifications and homogenous contrast enhancement in arterial phase (Fig. 14.18); when larger in size, the lesion can present central necrotic changes with fluid density. The margins are well circumscribed due to the presence of a capsule, and a peripheral rim of c.e. in arterial phase may be observed. This type of contrast enhancement allows differential diagnosis with cystic lesions of the pancreas. Typically, these tumors have a non-infiltrative growth pattern, and they cause displacement of adjacent structures. This type of growth allows differentiation from pancreatic ductal adenocarcinoma that has an infiltrative behavior. The arterial phase on CECT is mandatory to detect *pancreatic islet cell tumors* because in portal phase, they can

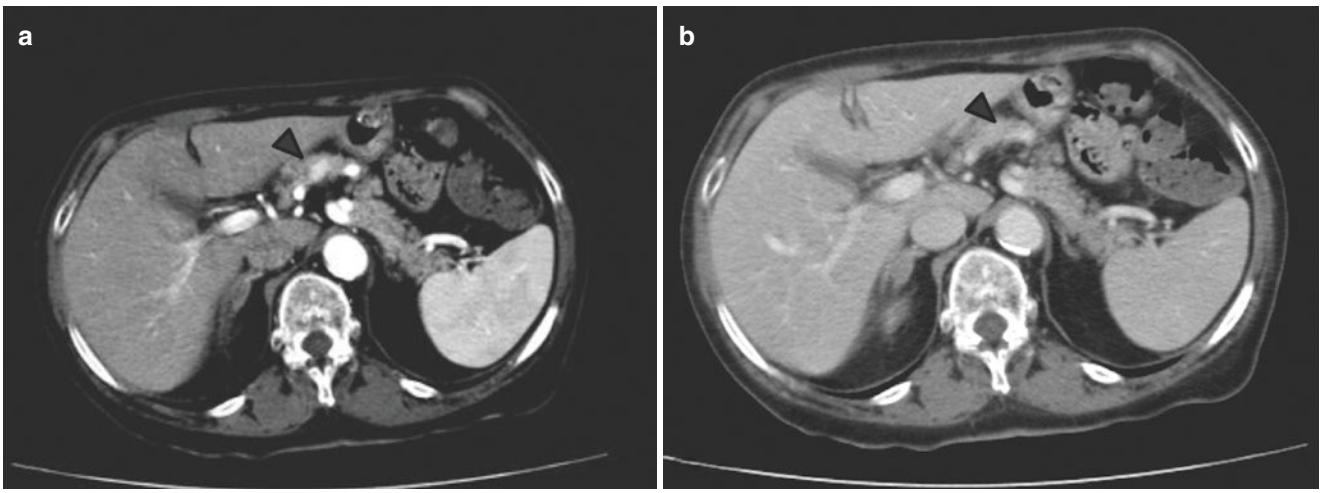

Fig. 14.18 Pancreatic carcinoid neoplasm. CECT on arterial phase (**a**): a hypervascular pancreatic lesion is seen (arrowhead). The lesion is not easily appreciable on portal phase (**b**)

be isointense compared to the rest of pancreatic parenchyma and small lesions may be missed.

Key Learning Points

- Pancreatic lesions can be divided into solid and cystic lesions.
- Regarding pancreatic cystic tumors, they can be divided into intraductal papillary mucinous neoplasms (IPMN), mucinous pancreatic cystadenomas, and pancreatic serous cystoadenomas.
- Pancreatic ductal adenocarcinoma is a malignant neoplasm that commonly occurs in the elderly. The typical locations of pancreatic ductal adenocarcinoma are the pancreatic head or the uncinate process. Pancreatic ductal adenocarcinoma commonly appears like an isodense mass on NECT, with heterogeneous poor contrast enhancement in particular in arterial phase on CECT.
- Endocrine tumors of the pancreas or pancreatic islet cell tumors are usually solitary, but they can be associated with MEN I, von Hippel-Lindau, or tuberous sclerosis. They can be classified as syndromic and non-syndromic, depending on whether or not they produce hormones.

14.11 Spleen

Lesions in the spleen can be categorized as benign (usually with fluid attenuation pattern) and malignant (most commonly solid). Splenomegaly is defined when the spleen is ≥13 cm in length: it may result from hematologic and lymphoproliferative disorders, infiltrative pathologies, vascular congestion, or infectious-inflammatory conditions.

Splenic infarction (usually triangular in shape), splenic cyst and splenic lymphangioma (with absent c.e. on CECT), and splenic abscess (low attenuation or absent c.e. lesions that may demonstrate peripheral rim) are the most common benign splenic lesions with near to fluid attenuation. Spleen hamartoma and spleen hemangioma are benign solid tumors. Spleen hemangioma has a contrast enhancement on CECT similar to that of liver hemangioma. The most common primary malignant tumors are lymphomas, which usually occur as hypovascular mass lesions in the portal phase, and angiosarcoma.

Spleen metastases usually appear as multiple solid lesions with hypovascular appearance in the portal phase. Splenic cystic metastases can be observed as secondary involvement from ovary, breast, or mucinous GI tumors.

Key Learning Points

- Spleen lesions can be categorized as benign (usually with fluid attenuation pattern) and malignant (most commonly solid).
- Splenomegaly is defined when the spleen is longer than 13 cm: it may result from hematologic conditions, lymphoproliferative disorder, infiltrative pathologies, vascular congestion, or infectious-inflammatory causes.

14.12 Adrenal Glands

Adrenal lesions are divided into benign and malignant. These lesions are recognized more often due to the increase of CT examinations. Adrenal lesions are often an incidental finding during a CT examination performed for other reasons. The radiologist plays a crucial role in the differential diagnosis of these lesions (Table 14.8).

Table 14.8 Flow chart of the differential diagnosis of adrenal lesions

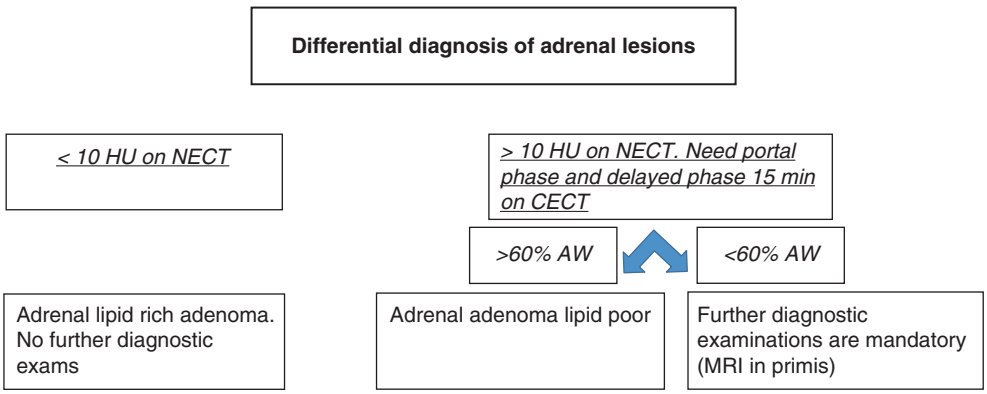

NECT non-contrast-enhanced CT, *AW* absolute washout

Adrenal adenomas are the most common incidental adrenal lesions. As a consequence, adrenal adenomas enter in differential diagnosis with adrenal metastases, particularly when a history of malignancy is present. Adrenal adenomas can be classified as functioning and non-functioning. Non-functioning adenomas constitute the majority of adrenal adenomas. Another possible classification divides them into typical and atypical adenomas: typical adenoma is <3 cm in diameter with a high content of fat tissue. The atypical adenoma is defined by the presence of hemorrhage, lack of fat tissue, necrosis, calcification, and larger size. When an adrenal lesion is larger than 4 cm, it has a high probability to be malignant. Typical adrenal adenomas are well-circumscribed lesions with a density inferior to 10 HU on NECT due to high lipid content ("lipid-rich" adenoma) (Fig. 14.19). When an adrenal lesion has a density >10 HU on NECT, contrast media administration is mandatory to differentiate them from metastases or other solid lesions. Adrenal washout is diagnostic for "lipid-poor" adenoma.

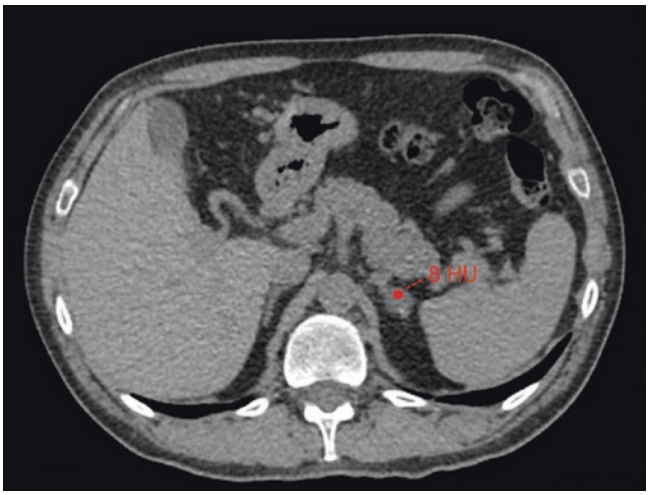

Fig. 14.19 Adrenal adenoma. NECT showing left adrenal gland with a round lesion demonstrating a density of 8 HU. The lesion's density is less than 10 HU. No further diagnostic work-up is needed, since the lesion can be classified as a lipid-rich adenoma

$$\text{NECT}\,(\text{HU}) - \text{delayed CECT after}\,15\,\text{min}\,(\text{HU}) \,/\, \text{CECT}\,(\text{HU})\,\text{in portal phase} \times 100$$
$$(\text{The result is the relative washout})$$

$$\text{CECT}\,(\text{HU})\,\text{in portal phase} - \text{delayed CECT after}\,15\,\text{min}\,(\text{HU}) \,/\, \text{CECT}\,(\text{HU})\,\text{in portal phase} - \text{NECT}\,(\text{HU}) \times 100$$
$$(\text{The result is the absolute washout})$$

$$\text{Relative washout} > 40\% \text{and absolute washout}\,(\text{AW}) > 60\% \text{ are diagnostic for adenoma.}$$

Adrenal carcinoma is rare and can be functioning or non-functioning depending on hormone secretion. When adrenal carcinomas are non-functioning, they can appear as large lesions. On CECT, the adrenal carcinoma appears as a solid mass with possible areas of necrosis (cystic appearance), hemorrhage, and calcifications. These lesions tend to infiltrate the liver, the inferior vena cava, and the kidney, based on their localization. In some cases, it is not possible to differentiate if the lesion originates from the liver or from the adrenal, especially if large in size.

Adrenal metastases are the most common adrenal malignant lesions and can be bilateral. The most frequent tumors that metastasise to adrenal glands are lung cancer, colorectal cancer, breast cancer, and pancreatic cancer. HCC and renal cancer may involve adrenal glands as well. It may be difficult to distinguish metastasis from "lipid-poor" adrenal adeno-

mas on CECT if a NECT and delayed phase are not acquired. Adrenal metastases are often round in shape, uni- or bilateral, with NECT value > of 10 UH and prolonged washout pattern (absolute washout value <60%).

Key Learning Points

- Adrenal lesions are often an incidental finding during a CT examination performed for other reasons.
- Adrenal adenomas can be classified as functioning and non-functioning. Non-functioning adenomas constitute the majority of adrenal adenomas. Another possible classification divides them into typical and atypical adenomas: typical adenoma is <3 cm in diameter with a high content of fat tissue.
- When an adrenal lesion has a density >10 HU on NECT, contrast media injection is mandatory to differentiate them from metastases or other solid lesions. Adrenal washout is diagnostic for "lipid-poor" adenoma.
- Adrenal metastases are the most common adrenal malignant lesions and can be bilateral. The most frequent tumors that metastasise to adrenal glands are lung cancer, colorectal cancer, breast cancer, and pancreatic cancer.

14.13 Kidney

Renal lesions can be divided into cystic and solid lesions. A diagnostic road map based on morphology, HU, and contrast enhancement behavior will be provided to perform a differential diagnosis for cystic renal findings (Table 14.9).

14.13.1 Renal Cystic Lesions

Renal cysts are the most common benign findings in the kidneys. Renal cysts can be divided into cortical and sinus cysts. Renal sinus cysts are benign. They can be subdivided into parapelvic cysts that originate from the adjacent parenchyma and protrude into the renal sinus and peripelvic cyst that originates within the sinus itself. If a renal cyst demonstrates no contrast enhancement or a difference in attenuation <10 UH from NECT to CECT (on portal phase), it is considered as non-enhancing simple cysts. If there is an increase in density from 10 to 20 HU, it is indeterminate, and pseudoenhancement artifact should be considered. A difference in density >20 HU is a major criterion to classify it as a complex cyst. Bosniak classification is helpful in predicting the risk of malignancy of a complex renal cyst. Simple cysts are well-defined, with thin or imperceptible wall, and they show water attenuation (<20 HU) on NECT. These cysts are classified as Bosniak I. When a cyst presents with minimally increased number of septa, but nonmeasurable c.e. of a hairline-thin septa, they are classified as Bosniak II. Hyper-attenuating cysts on NECT are well-capsulated cysts with thin or imperceptible hyper-attenuating (60–90 HU) walls and are classified as Bosniak II F. Strict follow-up is mandatory in II F cysts. Indeterminate cysts show thick margins, nodular multiple septa, or wall with measurable enhancement, hyperdense on CT (Bosniak III). These lesions have a high probability to be malignant

Table 14.9 Flow chart of the differential diagnosis of cystic renal lesions

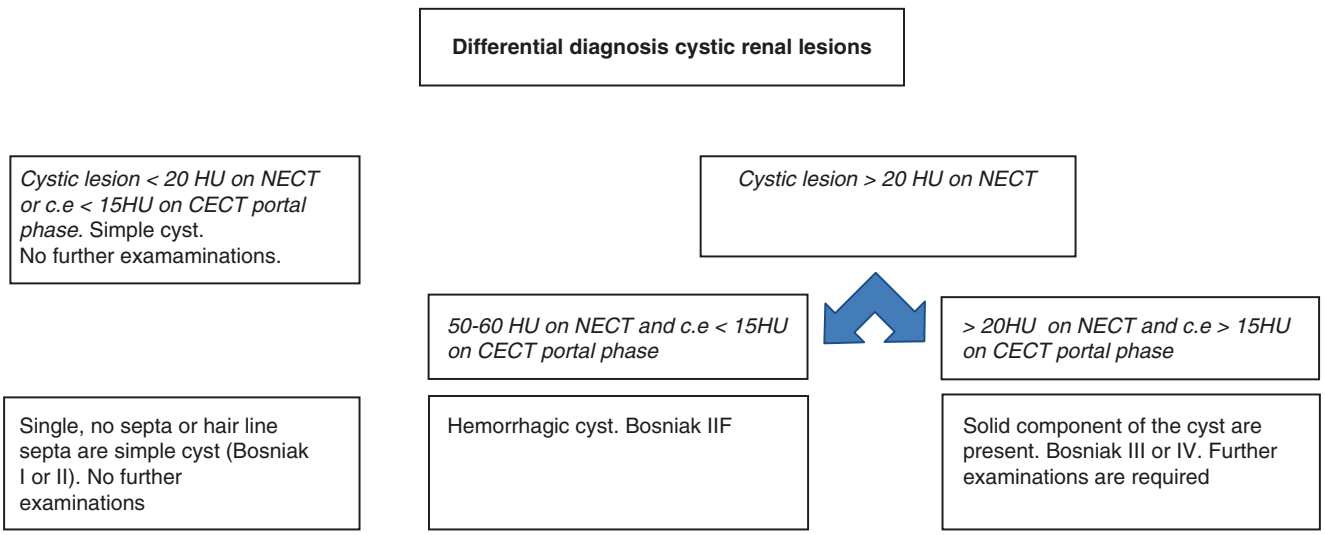

C.e. contrast enhancement

(50%). Malignant renal cysts are solid masses with a large cystic or a necrotic component (Bosniak IV) (Fig. 14.20).

14.13.2 Renal Non-Cystic Lesions

Renal lesions that do not exhibit a cystic density such as angiomyolipoma with negative densitometric values on NECT and solid lesions that frequently exhibit high UH values on NECT and contrast enhancement on CECT are also considered as solid findings. The most common renal non-cystic lesions are renal angiomyolipoma, renal cell carcinoma, and transitional cell carcinoma.

Renal angiomyolipoma: most lesions involve the cortex and demonstrate macroscopic fat content (less than −20 HU). When small in size, it can be difficult to differentiate them from a small simple cyst. Fat-containing lesions are not pathognomonic of renal angiomyolipoma because lipid necrosis or osseous metaplasia can be present also in renal cell carcinoma and metastasis. Multiple renal angiomyolipomas can be observed in tuberous sclerosis.

Renal cell carcinoma: it is the most common renal tumor. It is derived from tubular epithelium. Renal cell carcinoma most frequently occurs in middle-aged and elderly patients. Clinically it may manifest with flank pain or hematuria. Renal cell carcinomas, mostly when asymptomatic, are usually found as small incidental lesions. The recognized risk factors for kidney cancer are cigarette smoking, obesity, and dialysis-related cystic disease. Renal cell carcinoma shows soft tissue attenuation on NECT. Larger lesions can frequently have areas of necrosis or fat, and some calcification can be present. On CECT they demonstrate variable enhancement, usually less than the normal cortex. Large lesions have irregular enhancement due to areas of necrosis (Fig. 14.21). When the renal cell carcinoma is well capsulated and a pseudocapsule is present, the differential diagnosis with renal oncocytoma cannot be made. The clear cell subtype may show much stronger enhancement.

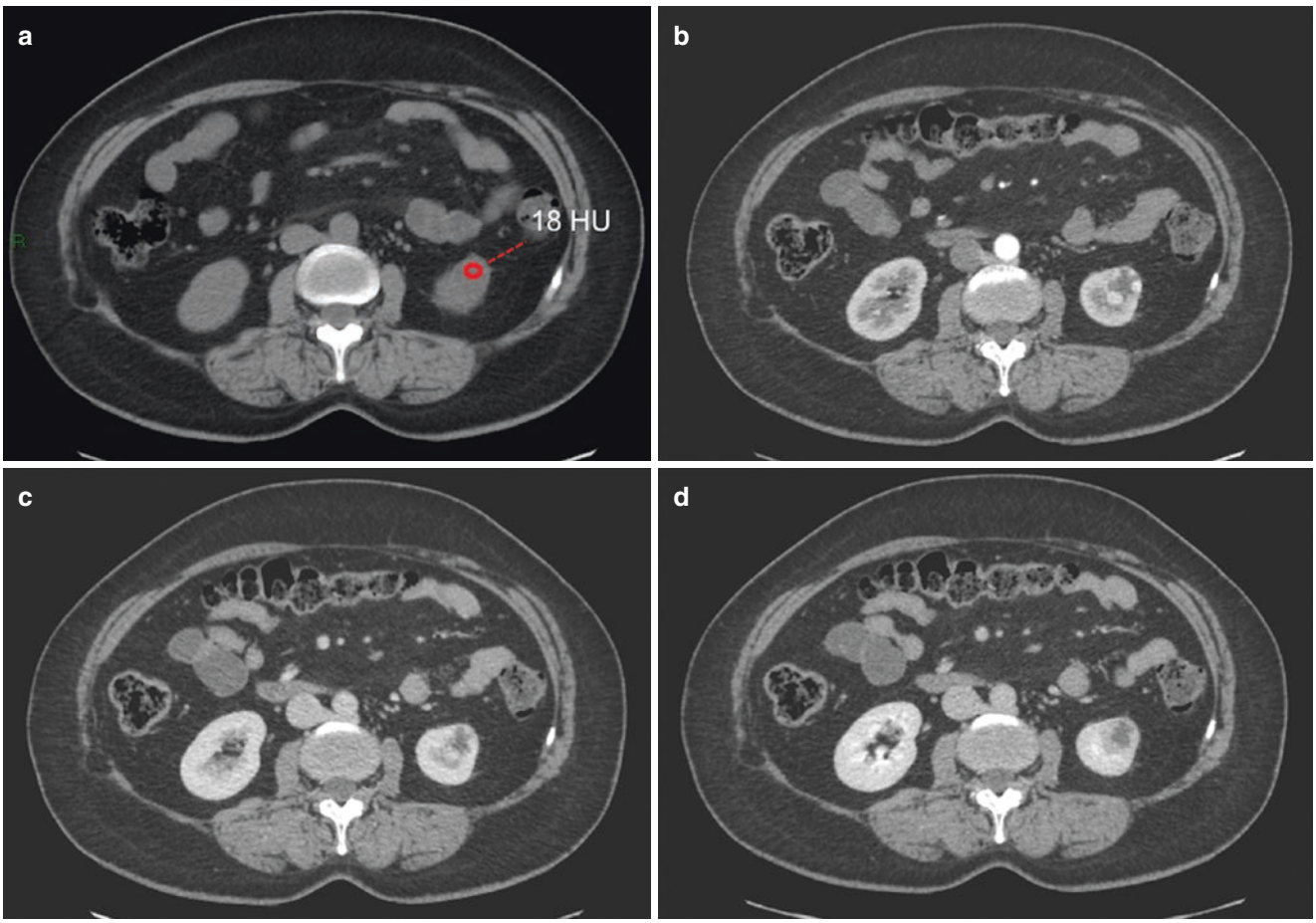

Fig. 14.20 Bosniak IV cystic lesion. NECT (**a**) showing a lower pole cystic lesion of the left kidney. The lesion's density is 18 HU, similar to fluid. CECT on arterial phase (**b**) and portal phase (**c**) showing small mural nodular lesions with strong contrast enhancement. Wall thickening is better appreciable on delayed phase (**d**)

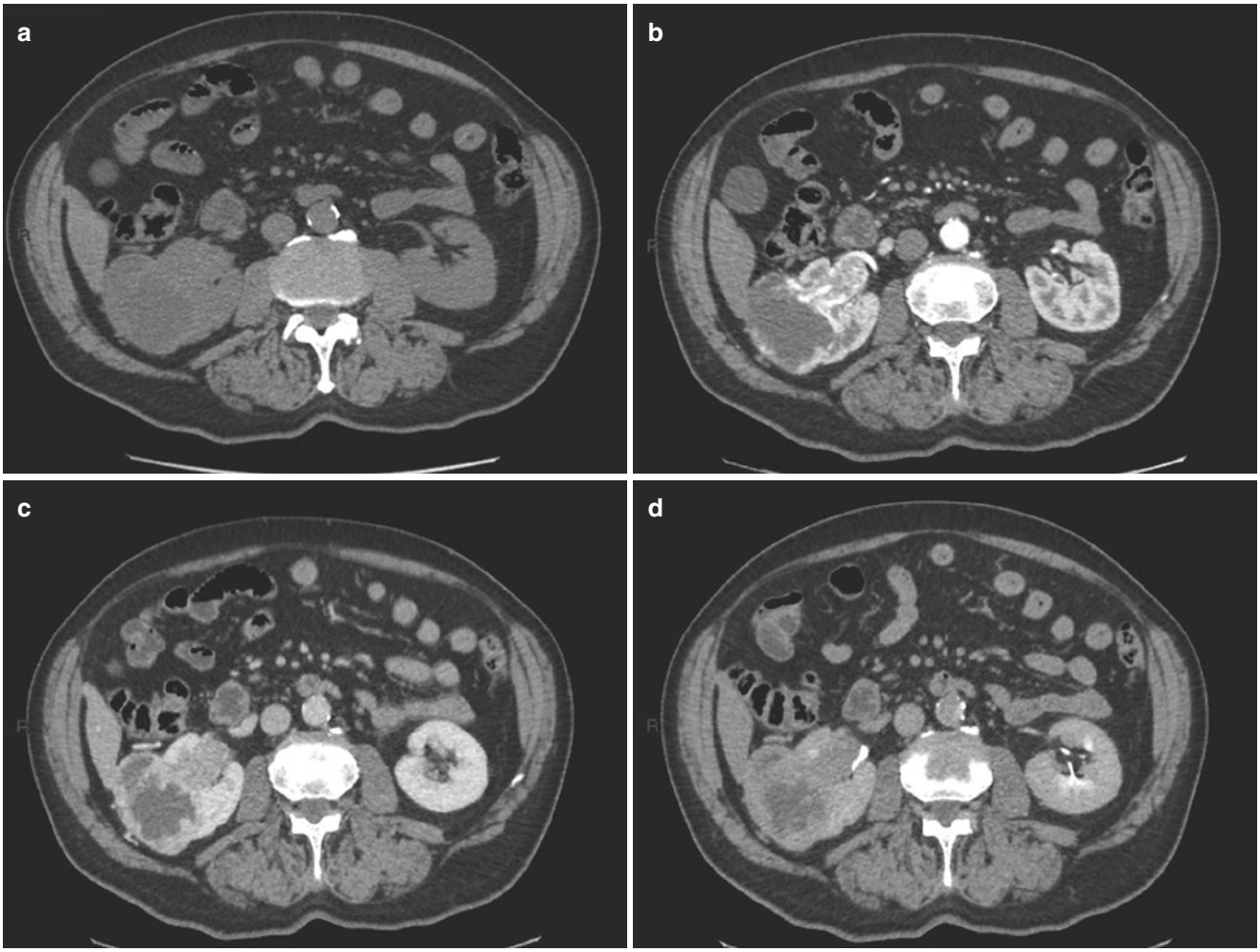

Fig. 14.21 RCC. NECT (**a**) shows a round lesion at the lower pole of the right kidney. The lesion has a large central necrotic component that is hypo-attenuating compared to the renal parenchyma with a peripheral rim of contrast enhancement on arterial phase (**b**). The delineation of viable tumor and necrosis is better seen on portal phase (**c**) and delayed phase (**d**)

Transitional cell carcinoma: it affects renal excretory pathways and may occur at the level of the calyx, pelvis, ureter, and bladder. Transitional cell carcinomas usually appear as papillary lesions that partly or completely occupy the excretory pathway. Another morphologic pattern of presentation is non-papillary type with nodular or sessile tumors. When transitional cell carcinoma grows into the renal pelvis, it can completely occupy the lumen and obliterate the renal sinus fat. Clinically, it presents frequently with micro- or macro-hematuria and pain at the side that mimics a renal colic when hydronephrosis is manifested as a result of obstruction. CT plays a fundamental role in the differential diagnosis between urinary stones and a neoplastic lesion. The diagnosis of obstructive renal calculus is already possible on the NECT phase where the presence of a hyper-attenuating calculus in the urinary tracts can be observed. In addition to the usual image CT protocol, it is crucial to perform scans between 5 and 10 min in which the contrast medium is excreted by the renal excretory system and fills the excretory tracts allowing the visualization of any filling defects. If a filling defect is present, it is necessary to evaluate whether this finding demonstrates contrast enhancement between the NECT phase and the arterial and portal phases. To increase sensitivity to detect transitional cell lesions, it is necessary to use a proper windowing by reducing the contrast and lowering the grayscale once delayed scans are obtained.

If the lesion to be studied is in the bladder, it is necessary to wait longer than 10 min after contrast administration to acquire the delayed phases. In this way we try to fill the bladder as much as possible with the contrast material especially for suspected anterior wall lesions. This is because the contrast material accumulates from the posterior bladder wall to the anterior wall due to gravity (Fig. 14.22). An anterior wall lesion can be studied also by positioning the patient prone on

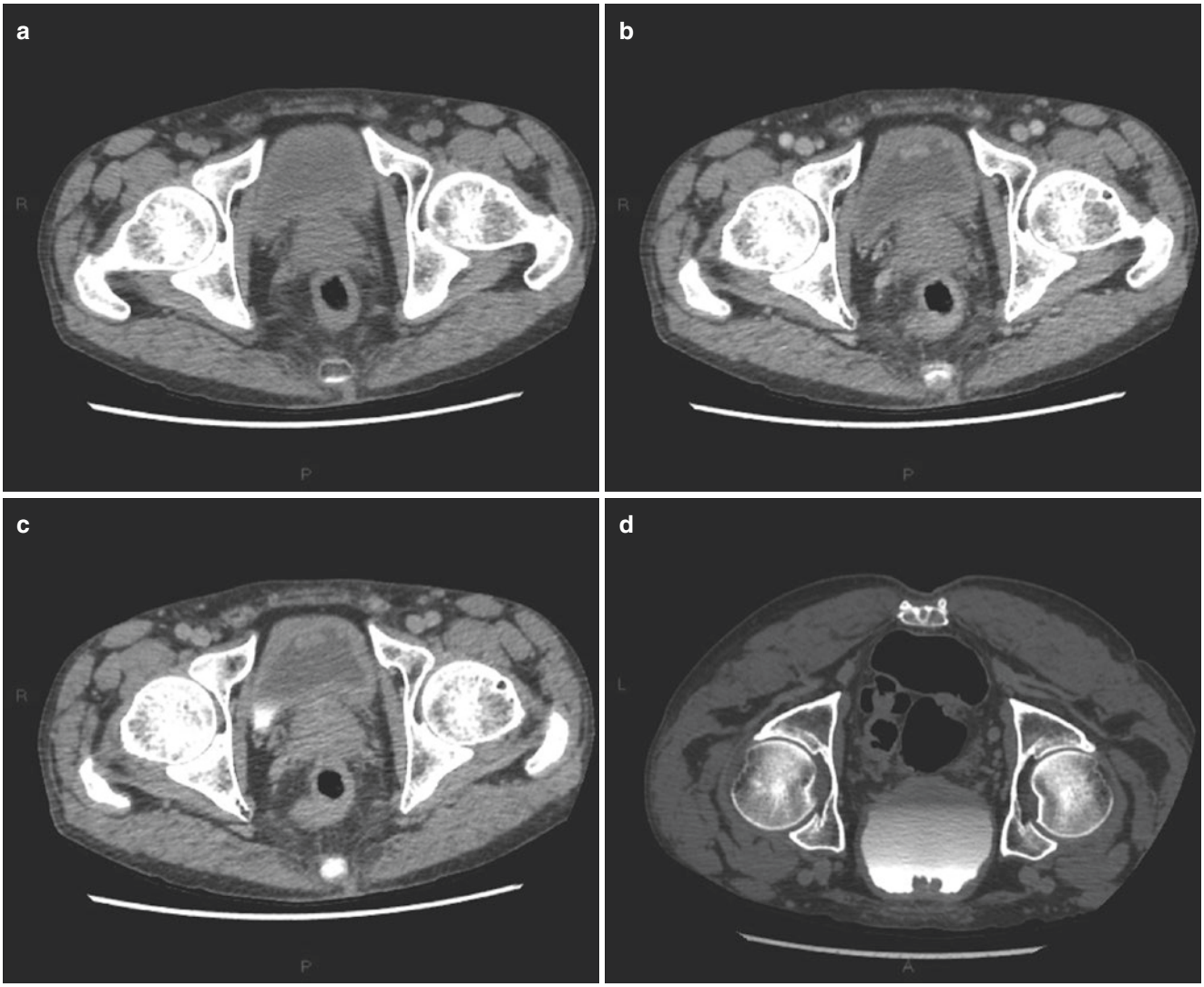

Fig. 14.22 Bladder polyps. Wall bladder thickness is measurable on NECT (**a**). On CECT portal phase, small pedunculated lesions on the bladder anterior wall are demonstrable (**b**). Mural nodular lesions cannot be clearly visualized on delayed phase (**c**) due to their anterior wall localization. CECT on delayed phase in prone position (**d**): wall nodular lesions appear as endoluminal filling defects

the bed during the delayed phase. When performing a study for the evaluation of a bladder lesion (observed by ultrasound or with cystoscopy), it is necessary to pay great attention to the entire urinary tract because transitional lesions are often multicentric (Table 14.9).

Key Learning Points

- Renal lesions can be divided into cystic and non-cystic (solid) lesions.
- Renal cysts are the most common benign finding in the kidneys. They can be divided into cortical and sinus cysts.
- Renal cell carcinoma is the most common renal tumor deriving from tubular epithelium. It most frequently affects middle-aged or advance-aged patients. It shows soft tissue attenuation on NECT. On CECT they demonstrate variable enhancement, usually less than the normal cortex. Large lesions have irregular enhancement due to areas of necrosis.
- Transitional cell carcinoma may usually appear as papillary lesions that partly or completely occupy the excretory tract lumen. CT plays a fundamental role in the differential diagnosis between urinary stones and neoplastic lesions.

14.14 Small Bowel Disease

The duodenum and small bowel can be studied on CECT using arterial and portal phase scans even after the oral administration of neutral contrast solution (used to distend the bowel lumen) that allows visualization of any defects of the intestinal mucosa. Multiplanar imaging also improved intestinal evaluation especially for the diagnosis of suspected obstruction. The most common pathologies of the small bowel including *congenital anomalies*, *neoplasms*, and *inflammatory diseases* will be discussed below.

The most frequently encountered *small bowel congenital anomalies* on an abdominal CT are duodenal diverticula, especially in the second and third portion of the duodenum, and Meckel's diverticulum.

Duodenal diverticula typically extend toward the pancreas, and their content are characterized by the presence of air bubbles and food residues. Duodenal diverticula may resemble cystic pancreatic lesions when air bubbles are absent, and the differential diagnosis between these two entities can be difficult: in these cases the oral positive contrast media may be helpful because if the contrast medium is able to fill the lesion, the diagnosis of duodenal diverticulum can be made. Meckel's diverticulum is the most common congenital abnormality of the gastrointestinal tract. The most frequent location of Meckel's diverticulum is 30 cm proximal to the ileocecal valve, but it can rarely be seen on CT examination due to the low difference in contrast compared to the small bowel. It can only be visualized when there is inflammation of the Meckel's diverticulum.

Small bowel neoplasms are relatively uncommon, and CT remains the modality of choice to identify them. The gastrointestinal stromal tumors (GIST) of the small bowel tend to be more aggressive than gastric cancers. GISTs tend to be round in shape and show heterogeneous contrast enhancement on CECT despite a central hypodense area due to necrosis. They are often exophytic even if intramural variants (or even polypoid variants) have been described (Fig. 14.23).

Carcinoid tumors or neuroendocrine tumors are the most common small bowel malignant neoplasm. They are derived from neuroendocrine cells in the submucosal wall, and are usually small in size and may not be localized during a CECT examination. When visible, neuroendocrine tumors show a hypervascular behavior. These lesions often affect mesenteric lymph nodes and show a desmoplastic reaction that retracts the mesentery and the small bowel loops.

Small bowel adenocarcinoma is rare, most likely occuring in the duodenum. The typical features on CECT are circumferential wall thickening that cause duodenum obstruction. When the small bowel adenocarcinoma involves the entire thickness of the bowel wall, mesenteric fat stranding can be observed. When a small bowel intussusception is present, an intestinal neoplasm should always be considered as the cause.

Risk factors for small bowel lymphoma include Crohn's and celiac disease. Lymphoma most frequently affects the distal region of the ileum and appears as a circumferential parietal thickening with intestinal pseudoaneurysm dilatation. Mesenteric lymphadenopathy and splenomegaly are also associated.

Even some *inflammatory diseases* such as Crohn's disease may affect the small bowel and in particular the distal

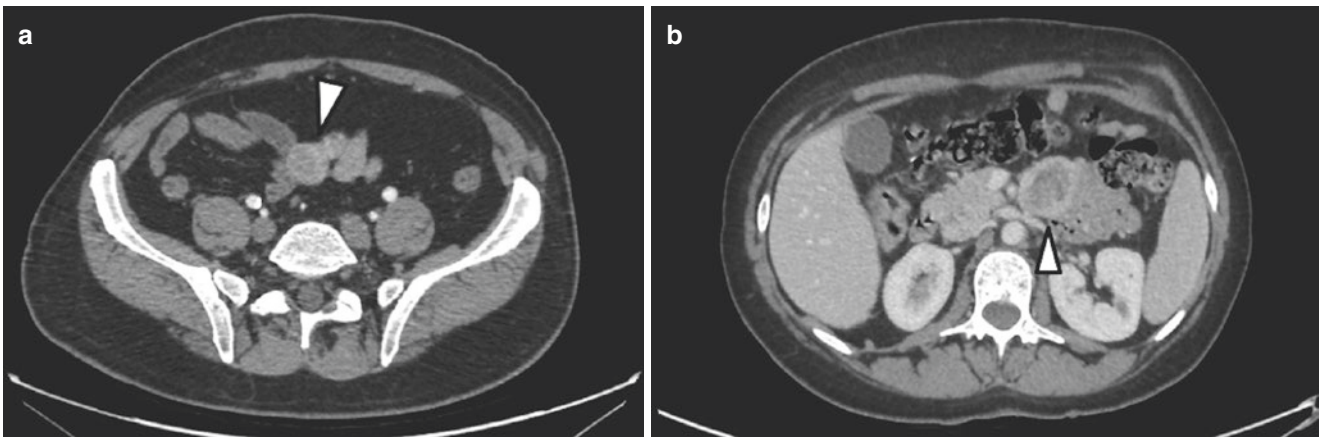

Fig. 14.23 GIST. CECT on portal phase (**a**) exhibits a round lesion arising from the wall of small bowel (arrowhead). The lesion shows a peripheral rim of contrast enhancement. Another example of GIST neoplasm that originates from the jejunum (arrowhead in **b**); a central area of necrosis can be observed

tract of the ileum. Although it is preferable to perform CECT examination with fluid distension of the intestinal loops using an oral contrast medium, it is also possible to observe the most common radiological signs of this pathology on CECT. In addition to the concentric thickening of the intestinal wall, CECT may demonstrate the fat stranding around the pathological mesenteric bowel loop, the "comb sing" due to increase of mesenteric vessels, and the skip lesions.

Key Learning Points

- The duodenum and small bowel can be studied on CECT using arterial and portal phase scans even after oral administration of neutral contrast solution (used to perform bowel lumen distension) to allow visualization of any defects of the intestinal mucosa.
- The most frequently encountered small bowel congenital anomalies on an abdominal CT are duodenal diverticula, especially in the second and third portion of the duodenum, and Meckel's diverticulum.
- Small bowel neoplasms are relatively uncommon, and CT remains the modality of choice to identify them.
- Carcinoid tumors or neuroendocrine tumors are the most common small bowel malignant neoplasm. They derive from neuroendocrine cells in the submucosal wall, and they usually are small in size and may not be localized during a CECT examination. When visible, neuroendocrine tumors show a hypervascular behavior.
- Some inflammatory diseases such as Crohn's disease may affect the small bowel and in particular the distal tract of the ileum. CECT examination with fluid distension of the intestinal loops using an oral contrast media is preferable.

14.15 Colorectal Cancer

Colorectal cancer is the most common tumor of the gastrointestinal tract. It most frequently affects the rectum, then the cecum and ascending colon, while transverse and descending colon tracts are less commonly involved. The most important acquired risk factors are related to a fat-rich diet, chronic inflammatory bowel disease, obesity, asbestos exposure, pelvic irradiations, and family history of benign or malignant colonic lesions. Some hereditary syndromes such as familial adenomatous polyposis syndrome (FAP), Peutz-Jeghers syndrome, and hereditary nonpolyposis colon cancer syndrome (HNPCC) may lead to colorectal carcinoma development.

Colorectal cancer may appear as a polypoid adenomatous lesion that progressively develops genetic mutations that lead to neoplastic transformation. Furthermore, colorectal cancer may appear as a protruded lesion (pedunculated, subpedunculated, and sessile) or as a flat lesion that can be observed only on virtual or optical colonoscopy. When colorectal cancer is found in advanced stage of illness, it often shows circumferential wall involvement. Ulcerated lesions may also be observed.

The clinical presentation of this disease can be subtle because if there is no rectal bleeding, colorectal cancer may not be found until it has reached a large size and intestinal obstruction or secondary involvement of other organs may be the first manifestations of the disease.

14.15.1 Morphologic Patterns of Presentation

Colorectal cancer may appear as a mass that narrows the bowel lumen with soft tissue density on NECT and strong contrast enhancement on CECT. Ulcerations and shouldering of the lesions margins may be observed in a large mass. Mucinous type tumors more frequently appear more hypodense due to mucus accumulations. Tumors with extraparietal extensions are commonly associated with perivisceral fat stranding and perivisceral enlarged lymph nodes.

Conventional CT has a low sensitivity to visualizing colonic lesions without proper intestinal preparation including gas bowel insufflation and antispastic medication. The stools inside the intestinal lumen and intestinal peristalsis decrease the ability to diagnose these lesions in their early stages. CT is therefore used for regional and systemic staging of intestinal cancer. When cancer affects the rectum, MRI is recommended for local staging, due to its greater sensitivity and specificity in the study of the rectal wall and soft tissues (mesorectal space).

Colorectal cancer in advanced stages is often associated with the presence of pathological lymph nodes that show a characteristic spread along the lymphatics associated with the arterial supply of the affected intestinal tract. For example, if cancer involves the rectum, pathological lymph nodes are more commonly those in the mesorectal space and belong to the lower mesenteric artery territory.

The most important CECT criteria to determine whether a lymph node is pathological is the size (in particular if the short axis of the lymph node exceeds 10 mm) and morphological criteria (the shape and the presence of a conserved

fatty sinus). Unfortunately, using these criteria, it is likely to underestimate the colorectal cancer due to low sensitivity and specificity. The risk of an underestimation can lead to incorrect management and may influence a patient's prognosis. MR and PET/CT are more accurate modalities in detecting the presence of colorectal cancer lymphadenopathies.

Key Learning Points

- Colorectal cancer is the most common tumor of the gastrointestinal tract.
- Colorectal cancer may appear as a mass that narrows the bowel lumen with soft tissue density on NECT and strong contrast enhancement on CECT. Ulcerations and shouldering of the lesions margins may be observed in a large mass. Tumors with extra-parietal extensions are commonly associated with perivisceral fat stranding and enlarged perivisceral lymph nodes.
- Conventional CT has a low sensitivity for visualizing colonic lesions without proper intestinal preparation including gas bowel insufflation and antispastic medication. When cancer affects the rectum, MRI is recommended for local staging, due to its greater sensitivity and specificity in the study of the rectal wall and soft tissues (mesorectal space).

14.16 Pelvic Lesions

Lesions of the male pelvis, such as prostate cancer, are not well appreciated on CT due to the poor contrast difference between tissues that decreases the sensitivity and specificity of the method. Therefore, only the most common female pelvic lesions are discussed here.

Ovarian lesions can be classified as benign or malignant and solid or cystic. The type of diagnostic and therapeutic approach changes in relation to the menopausal status of the patient. Cystic lesions, as in other parenchymal organs, are characterized by fluid attenuation (similar to water density from 0 HU to 10 UH). During menopause the ovaries generally decrease in size and are predominantly replaced by fibrotic tissue. In the premenopausal time, the ovaries have different morphology relating to the menstrual cycle.

The ovarian lesions have some characteristic CT patterns that can aid in categorizing the lesions as *simple cysts*, *hemorrhagic cysts*, *mature cystic teratomas* (dermoid cyst), and *other indeterminate cystic lesions*.

Simple cystic appearance lesions, particularly when single and from 3 to 7 cm in diameter, are commonly found in fertile women (derived from Graafian follicles), while cystic formations (in particular if large in size, with septa or nodules) in a menopausal woman, should be considered with suspicion. However, in postmenopausal women, small cystic lesion can be appreciated in the adnexa until 5 years after the menopausal onset.

Simple cystic lesion management is based on dimensional criteria and stratified for risk in accordance with premenopausal or postmenopausal status. In premenopausal women, a simple cyst from 3 cm to 5 cm in diameter must be mentioned in the CT report; a simple cyst with a diameter between 5 and 7 cm must be mentioned and should undergo ultrasound follow-up until it disappears; MRI and surgery are mandatory for a simple cyst with a diameter of > 7 cm. In postmenopausal women, simple cysts between 2 cm and 7 cm must be mentioned in the CT report, and a yearly follow-up with ultrasound should be performed; when simple cysts have a diameter >7 cm, further examinations are mandatory.

Hemorrhagic cysts show density values near to blood products (from 50 UH to 60 UH). If a hemorrhagic cyst in a premenopausal woman has a diameter of > 5 cm and remains unchanged after 1 year of follow-up, MRI examination must be performed. MRI or surgical evaluation is mandatory in women in early menopause with a hemorrhagic cyst of > 5 cm or for any hemorrhagic cyst in women in late menopause. Clot in hemorrhagic cysts may mimic a solid nodule, and, if visualized, a MRI exam should be performed.

The CT findings of *cystic mature teratoma* are a hypoattenuating unilocular mass near to fluid density in which a mural nodule (Rokitansky nodule) or calcifications can be observed. The presence of fat tissue (negative density values on ROI measurement) is pathognomonic for mature cystic teratoma diagnosis.

The *other indeterminate cystic lesions of the adnexa* are cystadenoma, cystadenofibroma, mucinous cystadenocarcinoma, and serous ovarian cystadenocarcinoma.

Cystadenoma and cystadenofibroma are benign ovarian neoplasms that can be serous (uniloculated) or mucinous (multiloculated). When these lesions are bigger than 7 cm in size, have multiple septa and demonstrable contrast enhancement on CECT, mural nodules showing contrast enhancement, and vascularized thick walls, they must be considered as having a high likelihood of neoplastic transformation. Mucinous ovarian cystadenocarcinoma and serous ovarian cystadenocarcinoma are the malignant variant. Advanced-stage ovarian tumors are often associated with the presence of ascites and peritoneal carcinomatosis, characterized by the thickened appearance of peritoneal sheaths or with small parietal nodules with demonstrable contrast enhancement.

Metastatic lesions of the ovaries are more often solid (Krukenberg metastases) and bilateral, but cystic metastases can also occur.

Key Learning Points

- Ovarian lesions have some characteristic CT patterns that can aid to categorize the lesions as a simple cyst, hemorrhagic cyst, mature cystic teratomas (dermoid cyst), and other indeterminate cystic lesions.
- Simple cystic lesion management is based on dimensional criteria and stratified for risk in accordance with premenopausal or postmenopausal status.
- The CT findings of cystic mature teratoma are a hypo-attenuating unilocular mass near to fluid density in which a mural nodule (Rokitansky nodule) or calcifications can be observed.
- The presence of fat tissue (negative density values on ROI measurement) is pathognomonic for mature cystic teratoma diagnosis.
- Metastatic lesions of the ovaries are more often solid (Krukenberg metastases) and bilateral, but cystic metastases can also occur.

14.17 Bone Lesions

Bone lesions can be divided into bone neoplasms, bone infections, bone-related lymphoproliferative disorders, bone-related endocrinological disorders, and miscellaneous. Bone neoplasms can be primary or secondary. Primary bone tumors can be classified in relationship to primary or secondary and with respect to the type of tissue: bone-, cartilage-, or fibrous forming tumors, bone marrow tumors, and miscellanea.

14.17.1 Primary Bone Lesions

The differential diagnosis of a primary bone lesion is heavily influenced by the age of the patient and the location.

Most likely malignant findings at CT are periosteal reaction (Codman's triangle), sunburst or lamellated periosteal reaction, cortical destruction, and soft tissue involvement. CT benign findings of periosteal reaction are well-defined margins and benign periosteal reaction (thick, continuous, or wavy periosteal thickening). Most radiological characteristics could overlap in many cases, so osteolytic or sclerotic type, age of patient, and site of the lesions can reduce the differential diagnosis. Bone tumor may appear as predominantly lytic lesions if bone destruction is predominant or sclerotic if new bone formation or tumor matrix calcifications are present.

Osteolytic lesions include the following:

Fibrous dysplasia or fibrous cortical defect, osteoblastoma, giant cell tumor, aneurysmal bone cyst, chondroblastoma or chondromyxoid fibroma, hyperparathyroidism (brown tumor), non-ossifying fibroma (NOF), enchondroma or eosinophilic granuloma, and simple (unicameral) bone cyst.

Sclerotic lesions include the following:

When solitary, the differential diagnoses include enostosis (bone island), osteosarcoma, chondrosarcoma, calcifying enchondroma, osteoblastoma, osteoid osteoma, Paget's disease, callus after fracture, and chronic osteomyelitis (Fig. 14.24). When sclerotic lesions appear as multifocal, the differential diagnoses include the metastasis from prostate and breast cancer, bone islands, hemangiomas (especially when located in the spine), multiple infarct (drugs related), and Paget's disease.

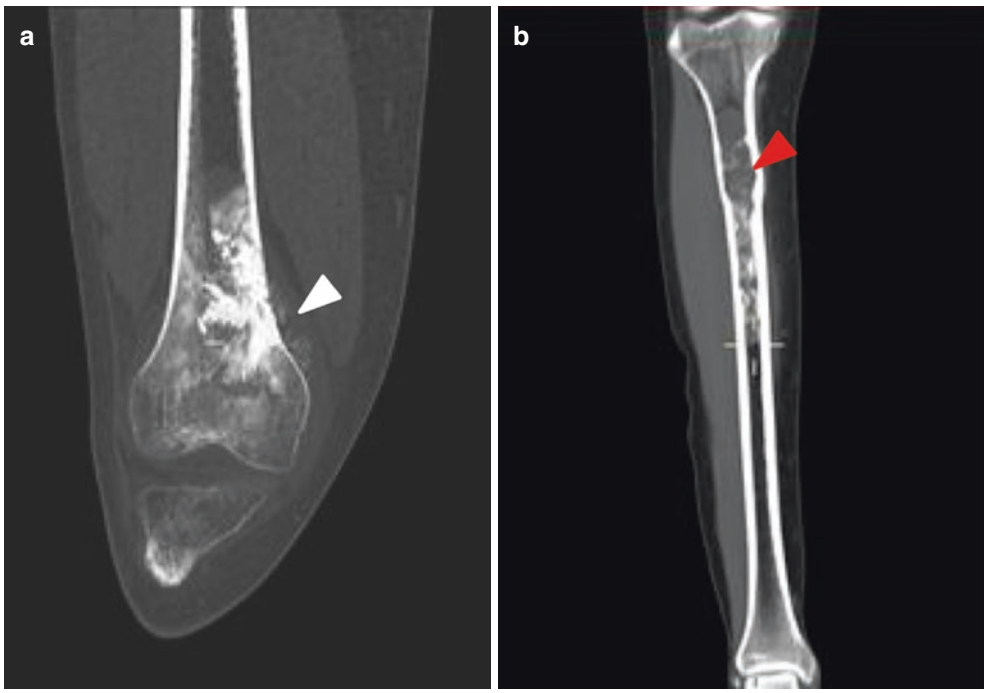

Fig. 14.24 Sclerotic primary bone tumor. NECT on coronal plane (**a**) shows a large sclerotic lesion in the diaphysis of the femur with a "sunburst" periosteal reaction (white arrowhead): the lesion resulted in osteosarcoma at biopsy. NECT on coronal plane (**b**) exhibit a large lesion with multiple calcifications and scalloped margins (red arrowhead). Low-grade chondrosarcoma was diagnosed at biopsy

14.17.2 Secondary Bone Lesions

Skeletal metastases account for 70% of all malignant bone neoplasms. Lung cancer, breast cancer, renal cell carcinoma, and prostate cancer account for approximately 80% of all skeletal metastases. Skeletal metastases tend to be multiple when present. The lymphoproliferative disorder may involve the bone usually as part of a disseminated process presenting as lytic infiltrative lesions (with permeative pattern) or bone sclerosis that may mimic other primary and secondary bone neoplasms on CT imaging. The pelvis and spine are commonly involved.

Skeletal metastases have three different patterns, depending on the preponderant process of bone resorption (osteolytic) or bone formation (osteoblastic) (Fig. 14.25) or mixed:

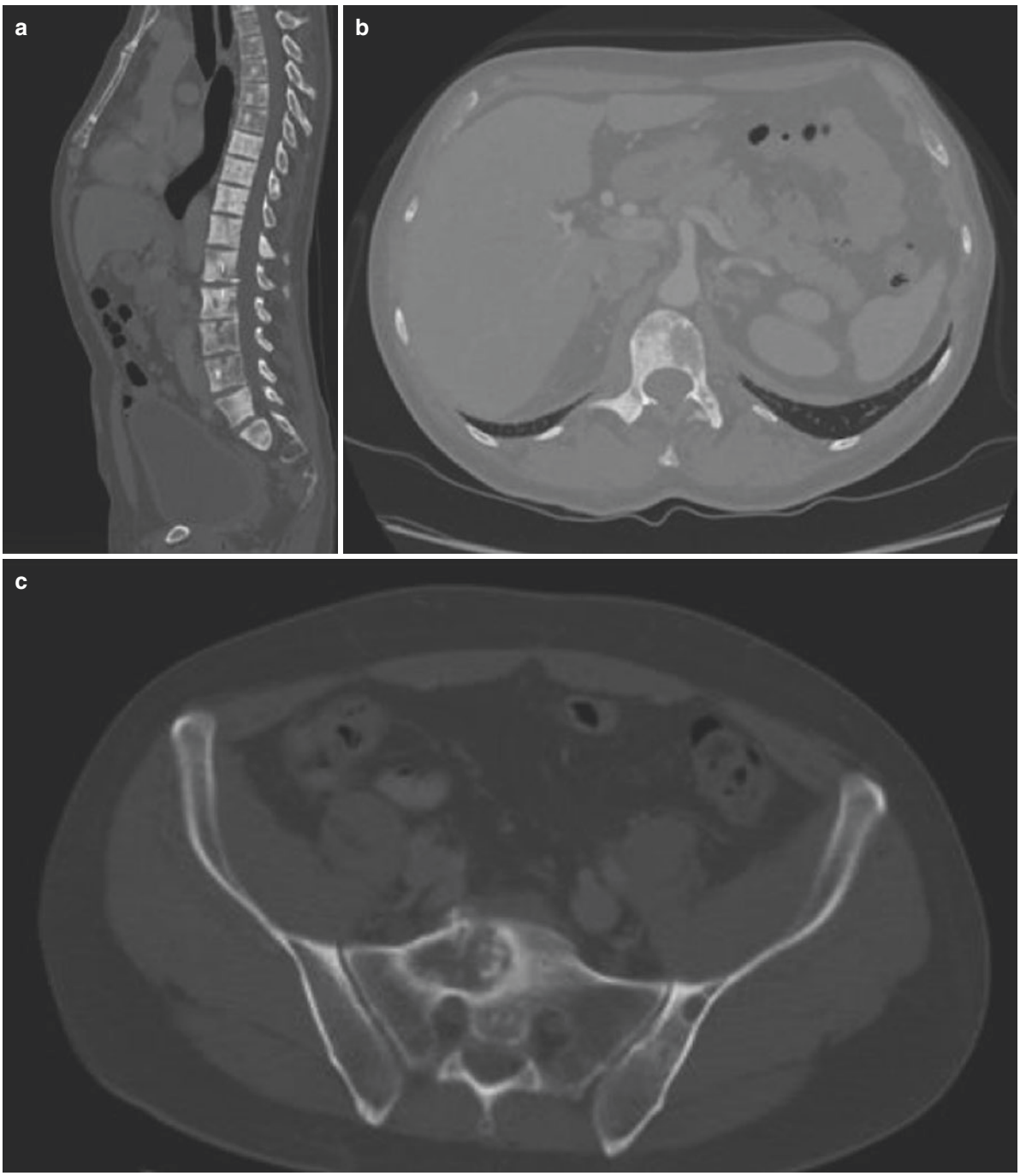

Fig. 14.25 Bone metastases. Sclerotic metastases from prostate carcinoma on dorsal and lumbar spine (**a**). Osteolytic metastases on dorsal spine (**b**) and sacrum (**c**) from lung adenocarcinoma

Osteolytic metastases are most likely due to thyroid cancer, lung cancer, renal cell cancer, gastrointestinal carcinomas, melanoma, hepatocellular carcinoma, and squamous cell carcinoma of the skin.

Sclerotic metastases are most likely due to prostate carcinoma, breast carcinoma (may be mixed), transitional cell carcinoma (TCC), carcinoid, medulloblastoma, neuroblastoma, mucinous adenocarcinoma of the gastrointestinal tract (e.g., colon carcinoma), and lymphoma.

Mixed lytic and sclerotic metastases are related to breast carcinoma and lung carcinoma; metastases from cervical cancer and testicular tumors are typically lytic but rarely can be mixed. Prostate carcinomas are typically sclerotic but can be mixed in a small fraction of patients.

14.17.3 Miscellaneous Bone Lesions

Paget's disease is a common, chronic bone disorder that leads to bone deformity. Paget's disease usually presents with all three types of bone alteration (sclerotic, lytic, and mixed) due to different amounts of osteoclastic or osteoblastic activity at different stages of disease: lytic form (initial active moment), mixed form (active form), and sclerotic form (late stage). When the spine is involved, the typical cortical thickening and sclerosis of subchondral and mural bone gives a "picture frame" appearance of the vertebral bodies. When the skull is involved, in the acute phase osteoporosis *circumscripta* (lytic lesion) may be observed. In long bones, the classic sign is the "candle flame sign" that is an area of a V-shaped lucency extending from the subchondral space toward the diaphysis.

*Infectious disorder*s: osteomyelitis is an infection of the bone most likely due to bacterial pathogens (pyogenic) or other pathogens such as tuberculosis, syphilis, or fungus. Osteomyelitis can be acute or chronic. In the acute phase (after 2 weeks), the most important CT findings are bone marrow lucency areas, cortical thickening with periosteal reaction (periostitis), and endosteal scalloping. In the chronic phase the most relevant sign is *sequestrum*. The cloaca sign may also be observed.

Involvement of the spine (spondylitis) by tuberculosis is also called Pott disease. Usually, both the vertebral body and the disk area are simultaneously affected by the disease. The most relevant findings on CECT are irregularity of affected vertebrae at the level of the end plates (initial phase), while extension into paravertebral soft tissue is more frequently observed in the late phase. Vertebra plana is a late finding in which the vertebra has completely lost its anterior and posterior height.

Key Learning Points

- The differential diagnosis of a primary bone lesion is heavily influenced by the age of the patient and the location. Most likely malignant findings on CT are periosteal reaction (Codman's triangle), sunburst or lamellated periosteal reaction, cortical destruction, and soft tissue involvement.
- Most radiological characteristics could overlap in many cases, so osteolytic or sclerotic type, age of patient, and site of the lesions can reduce the differential diagnosis.
- Skeletal metastases account for 70% of all malignant bone neoplasms. Lung cancer, breast cancer, renal cell carcinoma, and prostate cancer account for approximately 80% of all skeletal metastases. Skeletal metastases tend to be multiple when present.
- Osteolytic metastases are most likely due to thyroid cancer, lung cancer, renal cell cancer, gastrointestinal carcinomas, melanoma, hepatocellular carcinoma, and squamous cell carcinoma of the skin.
- Sclerotic metastases are most likely due to prostate carcinoma, breast carcinoma (may be mixed), transitional cell carcinoma (TCC), carcinoid, medulloblastoma, neuroblastoma, mucinous adenocarcinoma of the gastrointestinal tract (e.g., colon carcinoma), and lymphoma.
- Mixed lytic and sclerotic metastases are related to breast carcinoma, lung carcinoma (typically lytic but rarely can be mixed), carcinoma of the cervix, and testicular tumors. Prostate carcinomas are typically sclerotic but mixed in a small fraction of patients.
- Paget's disease is a common, chronic bone disorder that leads to bone deformity. Paget's disease usually presents with all three types of bone alteration (sclerotic, lytic, and mixed) due to different amounts of osteoclastic or osteoblastic activity at different stages of disease.

14.18 Abdominal Lymphadenopathies

CT interpretation criteria of lymphadenopathies: CT imaging for the assessment and characterization of pathological lymph node disease takes into account the size, the number, the morphology, the margins, the attenuation characteristics, and the enhancement after contrast.

Increase in size is not always pathologic, because often reactive nodes are bigger than 10 mm of transverse diam-

eter (considered as benign limit in size). Hyper-attenuating lymphadenopathy on NECT can be observed in Kaposi sarcoma, Castleman disease, carcinoid, and angioimmunoblastic lymphadenopathy. Calcifications are present in tuberculosis, sarcoidosis, lymphoma treated with radiotherapy, papillary thyroid carcinoma, and breast cancer. Lymph node metastatic disease commonly occurs along lymphatic pathways. For example, breast cancer tends to metastasize to axillary lymph nodes and rectal cancer to lymph nodes of the inferior mesenteric artery and mesorectal space.

Key Learning Point

- CT imaging for the assessment and characterization of pathological lymph node disease takes into account the size, the number, the morphology, the margins, the attenuation characteristics, and the enhancement after contrast.

Further Reading

Bernardino ME. Computed tomography of calcified liver metastases. J Comput Assist Tomogr. 1979;3:32–5.

Carter BW, Benveniste MF, Madan R, Godoy MC, de Groot PM, Truong MT, Rosado-de-Christenson ML, Marom EM. ITMIG classification of mediastinal compartments and multidisciplinary approach to mediastinal masses. Radiographics. 2017;37(2):413–36.

Chen IY, Kats DS, Jeffrey RB, et al. Do arterial phase helical CT image improve detection or characterization of colorectal liver metastases? J Comput Assist Tomogr. 1997;21(3):391–7.

El-Sherief AH, Lau CT, Wu CC, Drake RL, Abbott GF, Rice TW. International association for the study of lung cancer (IASLC) lymph node map: radiologic review with CT illustration. Radiographics. 2014;34(6):1680–91.

Erasmus JJ, Connolly JE, McAdams HP, Roggli VL. Solitary pulmonary nodules: Part I. Morphologic evaluation for differentiation of benign and malignant lesions. Radiographics. 2000a;20(1):43–58.

Erasmus JJ, McAdams HP, Connolly JE. Solitary pulmonary nodules: Part II. Evaluation of the indeterminate nodule. Radiographics. 2000b;20(1):59–66.

Grazioli L, Olivetti L, Fugazzola C, et al. The pseudocapsule in hepatocellular carcinoma: correlation between dynamic MR imaging and pathology. Eur Radiol. 1999;9:62–7.

Greenspan A, Jundt G, Remagen W. Differential diagnosis in orthopaedic oncology. Philadelphia: Lippincott Williams & Wilkins, c2007. (2006) ISBN:0781779308.

Helvie MA, Rebner M, Sickles EA, et al. Calcifications in metastatic breast carcinoma in axillary lymph nodes. AJR Am J Roentgenol. 1988;151(5):921–2.

Herts BR, Megibow AJ, Birnbaum BA, et al. High-attenuation lymphadenopathy in AIDS patients: significance of findings at CT. Radiology. 1992;185(3):777–81.

Hoang JK, Vanka J, Ludwig BJ, Glastonbury CM. Evaluation of cervical lymph nodes in head and neck cancer with CT and MRI: tips, traps, and a systematic approach. AJR Am J Roentgenol. 2013;200(1):W17–25.

Ichikawa T, Federle MP, Grazioli L, et al. Fibrolamellar hepatocellular carcinoma: imaging and pathologic findings in 31 recent cases. Radiology. 1999;213:352–61.

Itai Y, Matsui O. Blood flow and liver imaging. Radiology. 1997;202:306–14.

Jeung MY, Gangi A, Gasser B, Vasilescu C, Massard G, Wihlm JM, Roy C. Imaging of chest wall disorders. Radiographics. 1999;19(3):617–37.

del Pilar Fernandez M, Redvanly RD. Primary hepatic malignant neoplasms. Radiol Clin N Am. 1988;36:333–48.

Lucey BC, Stuhlfaut JW, Soto JA. Mesenteric lymph nodes: detection and significance on MDCT. AJR Am J Roentgenol. 2005;184(1):41–4.

Nasseri F, Eftekhari F. Clinical and radiologic review of the normal and abnormal thymus: pearls and pitfalls. Radiographics. 2010;30(2):413–28.

Nickell LT Jr, Lichtenberger JP 3rd, Khorashadi L, Abbott GF, Carter BW. Multimodality imaging for characterization, classification, and staging of malignant pleural mesothelioma. Radiographics 2014;34(6):1692-1706.

Nishino M, Ashiku SK, Kocher ON, Thurer RL, Boiselle PM, Hatabu H. The thymus: a comprehensive review. Radiographics. 2006;26(2):335–48.

Truong MT, Ko JP, Rossi SE, Rossi I, Viswanathan C, Bruzzi JF, Marom EM, Erasmus JJ. Update in the evaluation of the solitary pulmonary nodule. Radiographics. 2014;34(6):1658–79.

Whitten CR, Khan S, Munneke GJ, Grubnic S. A diagnostic approach to mediastinal abnormalities. Radiographics. 2007;27(3):657–71.